# PLOS COMPUTATIONAL BIOLOGY

# Role of the reaction-structure coupling in temperature compensation of the KaiABC circadian rhythm

Masaki Sasai [1,2,3]*

**1** Department of Applied Physics, Nagoya University, Nagoya, Japan, **2** Department of Complex Systems Science, Nagoya University, Nagoya, Japan, **3** Fukui Institute for Fundamental Chemistry, Kyoto University, Kyoto, Japan

* masakisasai@nagoya-u.jp

## Abstract

When the mixture solution of cyanobacterial proteins, KaiA, KaiB, and KaiC, is incubated with ATP in vitro, the phosphorylation level of KaiC shows stable oscillations with the temperature-compensated circadian period. Elucidating this temperature compensation is essential for understanding the KaiABC circadian clock, but its mechanism has remained a mystery. We analyzed the KaiABC temperature compensation by developing a theoretical model describing the feedback relations among reactions and structural transitions in the KaiC molecule. The model showed that the reduced structural cooperativity should weaken the negative feedback coupling among reactions and structural transitions, which enlarges the oscillation amplitude and period, explaining the observed significant period extension upon single amino-acid residue substitution. We propose that an increase in thermal fluctuations similarly attenuates the reaction-structure feedback, explaining the temperature compensation in the KaiABC clock. The model explained the experimentally observed responses of the oscillation phase to the temperature shift or the ADP-concentration change and suggested that the ATPase reactions in the CI domain of KaiC affect the period depending on how the reaction rates are modulated. The KaiABC clock provides a unique opportunity to analyze how the reaction-structure coupling regulates the system-level synchronized oscillations of molecules.

## Author summary

The reconstituted KaiABC circadian clock provides a unique opportunity to analyze how the effects of chemical and structural features of individual molecules determine the system-level oscillations of many molecules. By modeling the coupling of chemical reactions and structural transitions in the KaiC molecule, we showed that reducing the coupling strength enlarges the oscillation amplitude and period, explaining the observed striking change of the period length upon single-residue substitution in KaiC. We propose that thermal fluctuations attenuate the reaction-structure coupling similarly to the residue substitution, explaining the stable temperature compensation observed in the KaiABC clock.

The combined experimental and theoretical analyses should open a way to develop techniques to design the system-level molecular oscillations, further providing a basis for understanding circadian clocks in vivo.

## Introduction

The mixture solution of cyanobacterial proteins, KaiA, KaiB, and KaiC, shows the robust structural and chemical oscillations with the period of approximately 24 h when the solution is incubated with ATP in vitro [1–3]. This period is insensitive to the temperature change, showing the feature of temperature compensation [1]. An important question is whether this feature has a common molecular mechanism or the same mathematical principle as temperature compensation in generic transcription-translation oscillations (TTO). Circadian clocks in many organisms are driven by the time-delayed negative feedback in the TTO [4, 5], whose oscillation period is temperature compensated [6, 7]; the ratio of the period in 10˚C difference is $0.9 \lesssim Q_{10} \lesssim 1.1$, which is much closer to 1 than the value $\gtrsim 1.5$ expected from the temperature dependence of normal biochemical reactions. This temperature compensation has been studied with various theoretical models [8–19], but its mechanism remains a challenging problem.

There have been at least three views or approaches to temperature compensation; (i) the balance between opposing reactions, (ii) the correlation between oscillation period and amplitude, and (iii) the role of a critical reaction step. One view is the balance between reactions opposingly working to shorten or lengthen the period upon temperature change [7, 9]. Such balancing was mathematically formulated [20] and studied with different models [10–15]. In searching for the balancing reactions, various mechanisms were examined, including the balance between negative and positive feedback regulations [9] and the balance between ways of resetting bifurcations [12]. In particular, Lakin-Thomas et al. emphasized that the period length should correlate with the amplitude of oscillations [8], suggesting the possible use of the correlation as a clue to find the reactions responsible for the balance [17]. An alternative approach is to search for the critical reaction step or the molecule that determines temperature compensation. In mammals, phosphorylation of period 2 (PER2) regulated by casein kinase $I\varepsilon/\delta$ (CKI$\varepsilon/\delta$) is temperature insensitive [21], and this insensitivity was attributed to the reaction mechanism of the CKI$\varepsilon/\delta$ molecule [22].

Therefore, it is meaningful to analyze the temperature compensation of the KaiABC post-translational oscillations from the three views discussed for TTO. Previously, two hypotheses on the KaiABC temperature compensation were proposed based on the view (iii) of the critical reaction step and the view (i) on the balance between competing reactions. A critical reaction step is ATP hydrolysis in KaiC. KaiC hexamer is a slow ATPase, and variation of the ATPase activity among KaiC mutants is correlated with the variation of the oscillation frequency of those mutants [23, 24]. Because the ATPase activity of KaiC is temperature insensitive [23], this correlation suggested that ATPase activity determines temperature compensation in the KaiABC oscillations. In order to clarify whether such causality exists behind the observed correlation, further experimental and theoretical investigations are necessary. Another hypothesis was based on the assumption of balance among the competing binding reactions of KaiA to KaiC at different phosphorylation levels [25]. With this hypothesis, the population of KaiC at a highly phosphorylated state dominates in low temperature, which increases the free unbound KaiA molecules, and increases the overall binding rate of KaiA to compensate for the decrease of reaction rates at the low temperature. However, the accumulation of KaiC at a highly

phosphorylated state in low temperature was not observed experimentally [1]; therefore, exploration for other hypotheses and comparison among them are necessary.

Here, we propose a hypothesis based on the view (ii) of the correlation between oscillation period and amplitude. A recent experimental report revealed that substituting an amino-acid residue near the CI and CII domains interface in KaiC induces a striking change in the period from 15 h to 158 h with a suggested correlation between period and amplitude [26]. The modified period length in the mutant was anti-correlated with the volume of the residue after the substitution [26], indicating that the structural coupling between the CI and CII domains is crucial to determining the period; the period was enlarged when the structural coupling between domains was weaker with the smaller volume of residue at the domain interface. The recent X-ray analysis showed that KaiC undergoes structural transitions depending on the state of two phosphorylation sites in the CII and the nucleotide-binding state in the CI [27]. This observation indicated that the structural transitions of KaiC take place through the allosteric communication between CI and CII domains depending on the phosphorylation reactions in the CII and the ATPase reactions in the CI. On the other hand, the rates of those reactions should depend on the structure. Therefore, it is plausible to assume the feedback relations among reactions and structural transitions. Substituting smaller volume residue at the CI-CII interface should reduce the transition cooperativity and weaken the feedback coupling. The weakening of the negative feedback lengthens the period in general nonlinear oscillators as found in the TTO model [9]; therefore, the observed change in the mutants can be explained if the coupling among reactions and structural transitions of KaiC constitutes the negative feedback relation. Modifying strength of the negative feedback leads to the correlated change in amplitude and period in general nonlinear oscillators [9]. Ito-Miwa et al. compared five examples of the CI-CII interface mutations, showing two of them have smaller amplitude with shorter period [26], consistently with the negative-feedback hypothesis. However, the amplitude change of the rest three mutations was not sufficiently quantified [26], suggesting the need for the further statistical evaluation of the mutant oscillations.

In the present study, we propose that the structural coupling between the CI and CII is weakened through thermal fluctuations, weakening the negative feedback relations. In the higher temperature, the larger thermal fluctuations at the CI-CII interface should obscure the specific atomic interactions at the interface, producing a similar effect to the substitution to the smaller volume residue. This weakening of interactions at the interface reduces the negative feedback strength, enhancing the oscillation amplitude, lengthening the period, and compensating for the thermal acceleration of reactions in the higher temperature. We analyze this hypothesis with a model of the KaiABC oscillator and discuss possible tests of the model prediction. We also analyze the correlation between the ATPase reactions and the oscillation frequency to discuss the role of the ATPase reactions in the Kai system temperature compensation.

## Model

### Problems at two levels; the molecular and ensemble levels

In modeling the KaiABC oscillator, we need to analyze two mechanisms: how individual KaiC molecules oscillate and how oscillations of many KaiC molecules synchronize to generate the ensemble-level oscillations in solution. Many theoretical works focused on the latter question as the sequential change of phosphorylation level of individual KaiC molecules was assumed in advance; then, the synchronization was explained using various hypotheses [25, 28–39].

A plausible hypothesis is based on KaiA sequestration [25, 34–44]; the preferential KaiA binding to particular KaiC states sequestrates KaiA, reducing the KaiA binding rate in the

other KaiC states, leading to the accumulation of the population in those states, and producing coherent synchronizaed oscillations. This hypothesis is consistent with the experimental observation that the ensemble oscillations disappear when KaiA is too abundant in the solution [45]. Various states of KaiC were assumed as the KaiA-sequestrating states; some models assumed KaiA is sequestrated into the lowly phosphorylated KaiC in the phosphorylation (P) process [25, 34–36, 40] or in the dephosphorylation (dP) process [37, 38]. The other models assumed that KaiA is sequestrated by forming the KaiC-KaiB-KaiA complexes that appear during the dP process [39, 41–44]. The present author showed [44] that the assumption of the KaiA sequestration into the KaiC-KaiB-KaiA complexes quantitatively explains the experimental data on how the oscillations are entrained when two solutions oscillating at different phases are mixed [46].

In the present study, we use the hypotheses of the KaiA sequestration into the KaiC-KaiB-KaiA complexes to explain the synchronization. We also model the mechanism of how oscillations are driven in individual KaiC molecules. In this way, we address the questions extending over the two levels, the individual molecular level and the ensemble level, to analyze how the molecular-level feedback coupling determines the ensemble-level oscillations and temperature compensation.

## Feedback coupling of reactions and structural transitions at the molecular level

At the molecular level, KaiC forms a hexamer [47–49], which is denoted here by $C_6$. The KaiC monomer is composed of the N-terminal (CI) and C-terminal (CII) domains [50], which are assembled to the CI and CII rings in $C_6$ [49] (Fig 1). The NMR [51, 52], small-angle X-ray diffraction [53], biochemical analyses [54], and X-ray crystallography [27] showed the cooperative structural transitions of KaiC hexamer between two, the structure in the P phase and the structure in the dP phase. We use the order parameter $0 \leq X \leq 1$ to describe the transitions between two typical conformations and thermal fluctuations around each conformation. We write $X(k, t) \approx 1$ when the $k$th KaiC hexamer at time $t$ takes the structure in the P phase, and $X(k, t) \approx 0$ when it takes the structure in the dP phase.

In the present model, we consider that the structural state is a hub of multifold feedback relations among reactions and structural transitions (Fig 1). We describe individual KaiC molecules with the structural parameter $X$ and coarse-grained variables representing three types of reactions; (1) the binding/unbinding reactions of KaiA and KaiB to/from KaiC, (2) the P/dP reactions in the CII, and (3) the ATPase reactions in the CI. We consider that these three types of reactions directly or indirectly depend on $X$, and these reactions affect $X$, constituting the multifold feedback relations.

**Binding/unbinding reactions of KaiA and KaiB.** KaiA and KaiB bind/unbind to/from KaiC in a coordinated way [55–60]. The CII ring of a KaiC hexamer can bind a KaiA dimer during the P process to form $C_6A_2$ [36, 61]. The cryo-electron microscopy and mass-spectrometry showed that each CI domain can bind a KaiB monomer to form KaiC-KaiB complexes, further binding KaiA dimers to form KaiC-KaiB-KaiA complexes, $C_6B_iA_{2j}$ with $j \leq i \leq 6$ [60]. The stoichiometry $C_6B_iA_{2j}$ implies the large capacity of KaiC-KaiB-KaiA complexes to absorb KaiA molecules. We consider the probability of the $k$th KaiC hexamer forming $C_6A_2$ at time $t$, $P_{C_6A_2}(k, t)$, and the probability forming $C_6B_iA_{2j}$, $P_{C_6B_iA_{2j}}(k, t)$.

Binding/unbinding of KaiA to/from the CII has a timescale of seconds [36]. Because this kinetics is much faster than the other reactions in KaiC, we describe $P_{C_6A_2}$ with the quasi-equilibrium approximation, $P_{C_6A_2}(k, t) = x_A(t)g_{C:A}(k, t)P_{C_6B_0A_0}(k, t)$ with $g_{C:A}(k, t) = h_A(k, t)/f_A(k, t)$, where $x_A(t)$ is the concentration of free unbound KaiA dimer at time $t$. $h_A(k, t)$ and
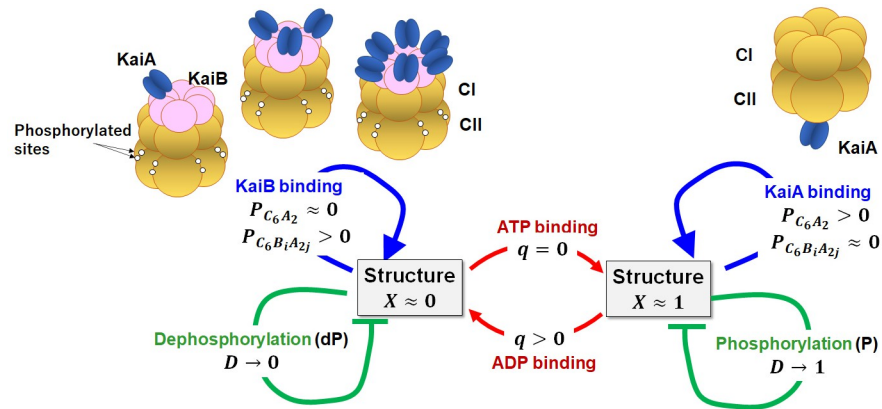
**Fig 1. Feedback coupling among reactions and structural transitions in KaiC hexamer.** The model is based on the fundamental experimental observations: KaiC forms a hexamer composed of the CI and CII rings. The CII has twelve sites to be phosphorylated. The KaiC hexamer undergoes allosteric transitions between two structures; the structure ($X \approx 1$) in the phosphorylation (P) phase and the structure ($X \approx 0$) in the dephosphorylation (dP) phase. A KaiA dimer can bind on the CII of the $X \approx 1$ KaiC with the probability $P_{C_6A_2}$, which promotes the P process to increase the phosphorylation level $D$. KaiB monomers can bind on the CI of the $X \approx 0$ KaiC, and a KaiA dimer can further bind on each KaiB monomer forming KaiC-KaiB-KaiA complexes with the probability $P_{C_6B_iA_{2j}}$ with $j \leq i \leq 6$. KaiA unbinds from the CII of the $X \approx 0$ KaiC, promoting the dP process to decrease $D$. Based on these observations, the model describes the feedback coupling in the KaiC hexamer by assuming (**i**) the KaiA binding on the CII stabilizes the $X \approx 1$ state, and (**ii**) the KaiB binding on the CI stabilizes the $X \approx 0$ structure. The assumptions (**i**) and (**ii**) account for the positive feedback to stabilize the $X \approx 1$ and $X \approx 0$ states. The model also assumes that (**iii**) the gradual rise of $D$ destabilizes the $X \approx 1$ structure and (**iv**) the gradual fall of $D$ destabilizes the $X \approx 0$ structure. The assumptions (**iii**) and (**iv**) support the time-delayed negative feedback to drive the transitions between the $X \approx 1$ and $X \approx 0$ states. The model further assumes (**v**) the stochastic ATP hydrolysis in the CI ($q \rightarrow 1$) destabilizes the $X \approx 1$ state, and (**vi**) the stochastic ADP release from the CI and the subsequent ATP binding ($q \rightarrow 0$) destabilize the $X \approx 0$ state. (**v**) and (**vi**) trigger the transitions between the $X \approx 1$ and $X \approx 0$ states. The assumptions (**i**) through (**vi**) generate the oscillations of individual KaiC hexamers. We hypothesized (**vii**) oscillations of multiple KaiC hexamers are coupled through the KaiA sequestration into the KaiC-KaiB-KaiA complexes, giving rise to the ensemble-level oscillations.

$f_A(k, t)$ are the binding and unbinding rate constants of a KaiA dimer to and from the CII, respectively. We represent the preferential KaiA binding to the $X \approx 1$ structure by assuming that $h_A(k, t)$ is an increasing function and $f_A(k, t)$ is a decreasing function of $X(k, t)$ (See Methods).

Binding/unbinding of KaiB has a timescale of an hour [36, 39]. We describe the slow temporal variation of $P_{C_6B_iA_{2j}}(k, t)$ by integrating the kinetic equations (Methods), which are represented with the rate constants of KaiB binding and unbinding, $h_B(k, t)$ and $f_B(k, t)$, respectively, and the rate constants of KaiA binding and unbinding to and from the KaiB, $h_{AB}$ and $f_{AB}$, respectively. We represent the tendency of preferential binding of KaiB to the $X \approx 0$ structure by assuming that $h_B$ is a decreasing function and $f_B$ is an increasing function of $X(k, t)$. Because KaiA does not directly interact with KaiC in this process, we assume $h_{AB}$ and $f_{AB}$ are independent of $X$. The unusually slow yet specific binding kinetics of the KaiB should be attributed to the fold transitions of KaiB. KaiB switches between ground state (KaiB$_{gs}$) and fold-switched state (KaiB$_{fs}$) by changing its secondary structures [62]. When only KaiB$_{fs}$ has a significant binding affinity to the CI and KaiB$_{fs}$ is the excited state with the activation energy of $\Delta E_{gs \rightarrow fs} > 0$, the small factor $\exp(-\Delta E_{gs \rightarrow fs}/(k_B T))$ explains the small $h_B$.

**P/dP reactions.** Each CII domain has two sites, Ser431 and Thr432, to be phosphorylated, which amounts to 12 sites in a KaiC hexamer. For simplicity, we do not distinguish Ser431 and Thr432 in the present expression, describing the phosphorylation level of 12 sites with the parameter $0 \leq D(k, t) \leq 1$; $D(k, t) = 1$ when 12 sites in the CII of the $k$th KaiC hexamer are all

phosphorylated, and $D(k, t) = 0$ when they are all unphosphorylated. Phosphorylation is promoted when KaiA binds on the CII [39, 55], and dephosporylation proceeds when it unbinds [39]. We represent this tendency by writing

$$\frac{d}{dt}D(k,t) = k_{\mathrm{p}}H^+(k,t)[1 - D(k,t)] - k_{\mathrm{dp}}H^-(k,t)D(k,t), \tag{1}$$

where $H^+(k, t) = z/(1 + z)$ and $H^-(k, t) = 1/(1 + z)$ represent the effects of binding and unbinding of KaiA with $z = P_{\mathrm{C_6A_2}}(k,t)/P_0$ and a constant $P_0$. For changing $D$ between 0 and 1 in $\sim$12 h, $k_{\mathrm{p}}$ and $k_{\mathrm{dp}}$ should be of the order of 0.1 h$^{-1}$.

**ATPase reactions.** Both CI and CII domains have ATPase activity, hydrolyzing about 10 ATP molecules in each CI domain and several ATP molecules in each CII domain in a day [23, 24]. It is reasonable to consider that ATP is consumed in the CII for supplying a phosphate group in the P process [40], but the reason for the ATP consumption in the CI has been elusive. With the present treatment $D(k, t)$ implicitly represents the ATPase reactions in the CII, and we more focus on the ATPase reactions in the CI. We consider the case ATP is abundant in the solution; therefore, the probability that the CI binds no nucleotide is small. Hence, we use the variable $q(k,t) = \frac{1}{6}\sum_{i=1}^{6} q(i; k, t)$ with

$$q(i; k, t) = \begin{cases} 1 & (i\text{th CI in the }k\text{th KaiC binds ADP}), \\ 0 & (i\text{th CI in the }k\text{th KaiC binds ATP}). \end{cases} \tag{2}$$

The ADP release and the subsequent ATP binding are the transition from $q(i; k, t) = 1$ to 0, and hydrolysis of the bound ATP is the transition from $q(i; k, t) = 0$ to 1. We simulate the stochastic ADP release and the ATP hydrolysis by treating $q(i; k, t)$ as a stochastic variable changing with the lifetime of the ADP bound state, $\Delta_{\mathrm{ADP}}$, and the frequency of hydrolysis, $f_{\mathrm{hyd}}$. The ATPase activity measured by the amount of the released ADP from KaiC is large in the P process [23], and the $X \approx 0$ ($X \approx 1$) structure binds ADP (ATP) [27]. These observations are consistent with the assumption that $f_{\mathrm{hyd}}$ is a constant independent of $X(k, t)$ and $\Delta_{\mathrm{ADP}}(k, t)$ is a decreasing function of $X(k, t)$. In practice, we represent this tendency as

$$\Delta_{\mathrm{ADP}}(k,t) = \Delta_{\mathrm{ADP}}^0[1 - \tanh((2X(k,t) - 1)/C_X)], \tag{3}$$

where $\Delta_{\mathrm{ADP}}^0$ is a constant determining the timescale and $C_X$ is a constant determining the seisitivity to the structure.

**Feedback coupling through structural change.** Allosteric transitions in protein oligomers typically have a timescale of $10^{-3} \sim 10^{-2}$ s [63], and we assume a similar timescale in the present problem. Because the other reactions in our system are much slower, we describe the KaiC structure as in quasi-equilibrium by treating the chemical states as the quasi-static constraints. Representing the constraints with a variable $R(k, t)$, we have the expression, $X(k, t) = \frac{1}{2}(1 + \tanh[R(k,t)/(k_{\mathrm{B}}T)])$ (See the Methods section). Here, the explicit form of $R(k, t)$ constitutes major assumptions on the feedback couplings in the present model. Expanding $R(k, t)$ up to the linear terms of $P_{\mathrm{C_6A_2}}$, $P_{\mathrm{C_6B_iA_{2j}}}$, $D(k, t)$, and $q(k, t)$, we have

$$R(k,t) = d_0 + d_1 P_{\mathrm{C_6A_2}}(k,t) - d_2 \sum_{i=0}^{6}\sum_{j=0}^{i} P_{\mathrm{C_6B_iA_{2j}}}(k,t)$$
$$-d_3[D(k,t) - (1 - D(k,t))] - d_4 F(q(k,t)), \tag{4}$$

where $d_0$ is a constant to determine the average structure, and $d_1$, $d_2$, $d_3$, and $d_4$ are constants defining the strength of the feedback coupling. We assume $d_1 > 0$, which stabilizes the $X \approx 1$

structure when KaiA binds on the CII, and $d_2 > 0$, which stabilizes the $X \approx 0$ structure when KaiB binds on the CI. Then, with the definitions of $h_A(k, t)$, $f_A(k, t)$, $h_B(k, t)$, and $f_B(k, t)$, we see that binding reactions constitute *the positive feedback loops* to stabilize the two states, the $X \approx 1$ and $X \approx 0$ states.

We use a constant $d_3 > 0$ in Eq 4, which destabilizes the $X \approx 1$ state when phosphorylated ($D \approx 1$) and destabilizes the $X \approx 0$ state when dephosphorylated ($D \approx 0$). This assumption is consistent with the X-ray crystallography analysis that Ser431 is phosphorylated in the $X \approx 0$ structure while dephosphorylated in the $X \approx 1$ structure [27]. Increase in $D$ from $D \approx 0$ to $\approx 1$ is promoted by the KaiA binding to the CII of KaiC, which is promoted in the $X \approx 1$ state, which then destabilizes the $X \approx 1$ state through the $d_3$ term. Decrease in $D$ from $D \approx 1$ to $\approx 0$ is promoted by the KaiA unbinding from the CII of KaiC, which is promoted in the $X \approx 0$ state, which then destabilizes the $X \approx 0$ state through the $d_3$ term. Therefore the $d_3 > 0$ in Eq 4 constitutes the negative feedback loops. Because $k_p$ and $k_{dp}$ in Eq 1 are small, this destabilization of $X$ is a slow process gradually proceeding after the structural transition. Therefore, the $d_3$ term represents *the time-delayed negative feedback loops* to drive the oscillations between the $X \approx 1$ and $X \approx 0$ states.

$d_4 F(q(k, t))$ in Eq 4 represents the coupling of structure with the ATPase reactions, which largely determines the balance between positive and negative feedback effects. This coupling was inferred from the observations that the ATP hydrolysis is necessary for binding KaiB to KaiC [51, 54, 64, 65], and that the structure is modified upon ATP hydrolysis [24, 27, 60, 66]. With $F(q(k, t)) = q(k, t)X(k, t) - (1 - q(k, t))(1 - X(k, t))$ and $d_4 > 0$, the ADP binding on the CI destabilizes the $X \approx 1$ state, while the ATP binding destabilizes the $X \approx 0$ state. Therefore, the stochastic ATP hydrolysis triggers the transition to the $X \approx 0$ state, and the stochastic release of ADP with the subsequent ATP binding triggers the transition to the $X \approx 1$ state (Fig 1).

Thus, the model describes the positive feedback between the structure and the binding/unbinding of KaiA and KaiB to/from KaiC (the $d_1$ and $d_2$ terms), the negative feedback between the structure and the P/dP process (the $d_3$ term), and the transition-triggering effects of the ATPase reactions (the $d_4$ term). These couplings generate the cooperative chemical and structural oscillations in individual KaiC molecules.

## Communication among many KaiC molecules at the ensemble level

We simulated the ensemble of $N = 1000$ or $2000$ KaiC hexamers. For $N = 1000$ and $V = 3 \times 10^{-15} l$, the concentration of KaiC is $C_T = 3.3 \ \mu M$ on a monomer basis, which is near to the value $3.5 \ \mu M$ often used in experiments. We assumed the ratio $A_T : B_T : C_T = 1 : 3 : 3$ as used in many experiments [23, 54, 67], where $A_T$ and $B_T$ are total concentrations of KaiA and KaiB on a monomer basis. The system was described by variables, $P_{C_6 A_2}(k, t)$, $P_{C_6 B_i A_{2j}}(k, t)$, $D(k, t)$, $X(k, t)$, $q(k, t)$, $x_A(t)$ and $x_B(t)$, with $k = 1, \ldots, N$. $P_{C_6 B_i A_{2j}}(k, t)$ and $D(k, t)$ were calculated by numerically integrating the kinetic equations, and $P_{C_6 A_2}(k, t)$ and $X(k, t)$ were calculated with the quasi-equilibrium approximation at each time step. $q(k, t)$ was calculated by simulating the stochastic transitions of $q(i; k, t)$ between 0 and 1 with frequencies $\Delta_{ADP}^{-1}$ and $f_{hyd}$. Concentrations of free unbound KaiA dimer and KaiB monomer, $x_A(t)$ and $x_B(t)$, were calculated at each time step from the following equations of conservation,

$$x_A(t) \quad + \quad \frac{1}{V} \sum_{k=1}^{N} P_{C_6 A_2}(k, t)$$

$$+ \quad \frac{1}{V} \sum_{k=1}^{N} \sum_{i=1}^{6} \sum_{j=1}^{i} j P_{C_6 B_i A_{2j}}(k, t) = A_T/2, \tag{5}$$

and $x_B(t) + \frac{1}{V}\sum_{k=1}^{N}\sum_{i=1}^{6} iP_{C_6B_i}(k,t) = B_T$. Competition between the 2nd and 3rd terms of the l.h.s. of Eq 5 provides communication among KaiC molecules leading to the synchronization. See the Methods section for details.

## Results

### Single-molecule and ensemble-level oscillations

Fig 2 shows the calculated example oscillations. A KaiC hexamer arbitrarily chosen from the simulated ensemble of $N = 1000$ hexamers shows the structural transitions between the states $X(k,t) \approx 1$ and $X(k,t) \approx 0$ (Fig 2A). The nucleotide-binding state in the CI ring $q(k,t)$ also exhibits transitions between the state rapidly fluctuating around $q(k,t) \approx 0.3$ and the state around $q(k,t) \approx 0.6$. The phosphorylation level $D(k,t)$ follows these switching transitions with the slower rates of the P/dP reactions; $D$ increases in the $X \approx 1$ state and decreases in the $X \approx 0$ state, showing saw-tooth oscillations.

At the ensemble level, these fluctuating oscillations in individual molecules are averaged, resulting in the regular oscillations of $\bar{D}(t) = \frac{1}{N}\sum_{k=1}^{N} D(k,t)$, $\bar{X}(t) = \frac{1}{N}\sum_{k=1}^{N} X(k,t)$, and $\bar{q}(t) = \frac{1}{N}\sum_{k=1}^{N} q(k,t)$ (Fig 2B). The ensemble-averaged rate of the ADP release from KaiC, $\bar{q}_r(t)$ (Methods), is large during the P phase as observed experimentally [23], and the ADP binding probability $\bar{q}(t)$ is large during the dP phase consistently with the experimental observations [27]. In this way, the model reproduces the stable circadian oscillations at the ensemble level averaging the synchronized individual KaiC oscillations.

### Modifications of the feedback strength

The binding of KaiA or KaiB may induce the global change of each KaiC subunit, shifting the position and orientation of subunit, whose effects represented by $d_1$ and $d_2$ in Eq 4 should be insensitive to the single-residue substitution at the CI-CII interface. On the other hand, P/dP in the CII or the ATPase reaction in the CI is the local atomic change around the phosphate group, whose effects are transmitted through chains of electrostatic and volume-excluding interactions, producing the allosteric communication between the CI and CII [27, 66]. This process should be sensitive to the atomic interactions at the CI-CII interface and hence sensitive to the single-residue substitution. Here, we assume that substituting a CI-CII interface residue to the smaller volume one is represented by the decrease in $d_3$ and $d_4$ in Eq 4 with a scaling factor $s < 1$ to $sd_3$ and $sd_4$ while $d_1$ and $d_2$ in Eq 4 being kept in their original values. With $s < 1$, the simulated phosphorylation level oscillations indeed show the large amplitude and long period as expected from the decrease in the negative feedback strength, while the
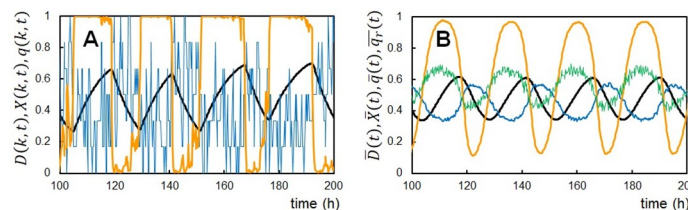


**Fig 2. Example oscillations of the simulated KaiABC system.** (**A**) The singlel-molecule oscillations of the phosphorylation level $D(k,t)$ (black), the structural state $X(k,t)$ (orange), and the ADP binding probability on the CI $q(k,t)$ (blue) of an arbitrarily chosen $k$th KaiC hexamer. (**B**) The ensemble-averaged oscillations of the phosphorylation level $\bar{D}(t)$ (black), the structural state $\bar{X}(t)$ (orange), the binding probability of ADP on the CI $\bar{q}(t)$ (blue), and the ATPase activity measured by the amount of the released ADP $\bar{q}_r(t)$ (green). $N = 1000$ at temperature $T_0 = 30°C$.
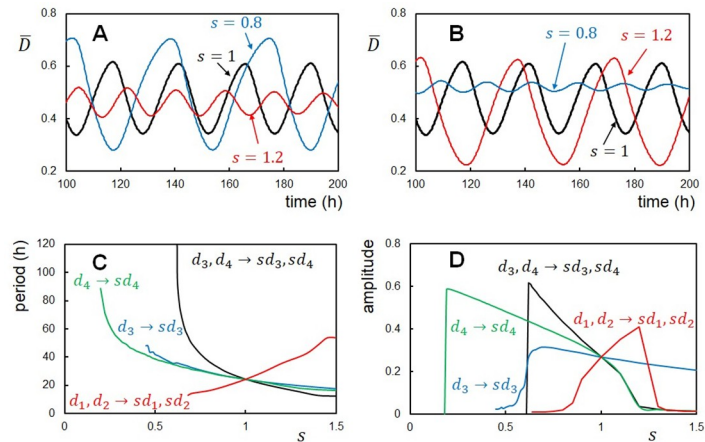
**Fig 3. Effects of modification of the reaction-structure feedback strength.** (**A**) and (**B**) Example oscillations of the ensemble-averaged phosphorylation level $\bar{D}(t)$ with a varying factor $s$. (**A**) The negative feedback coupling between structure and reactions was modified; the coupling with the P/dP reactions $d_3$ and the one with the ATPase reactions $d_4$ were modified to $sd_3$ and $sd_4$ with $s$ = 0.8 (blue), 1.0 (black), and 1.2 (red). (**B**) The positive feedback coupling between structure and the binding/unbinding reactions was modified; the coupling with the KaiA binding/unbinding $d_1$ and the one with the KaiB binding/unbinding $d_2$ were modified to $sd_1$ and $sd_2$ with $s$ = 0.8 (blue), 1.0 (black), and 1.2 (red). Period (**C**) and amplitude (**D**) of the simulated $\bar{D}(t)$ oscillations plotted as functions of the scaling factor $s$ for modifying $d_3$ to $sd_3$ while $d_1$, $d_2$, and $d_4$ being kept constant (blue), $d_4$ to $sd_4$ while $d_1$, $d_2$, and $d_3$ being kept constant (green), $d_3$ and $d_4$ to $sd_3$ and $sd_4$ while $d_1$ and $d_2$ being kept constant (black), and $d_1$ and $d_2$ to $sd_1$ and $sd_2$ while $d_3$ and $d_4$ being kept constant (red). $N$ = 1000 and temperature was $T_0$ = 30°C.

amplitude is small and the period is short for $s > 1$ (Fig 3A). On the contrary, with positive feedback enhancement with a scaling factor $s > 1$, changing $d_1$ and $d_2$ to $sd_1$ and $sd_2$ enlarges the amplitude and period, while they are reduced when $s < 1$ (Fig 3B).

These effects of the feedback strength modifications were systematically examined in Fig 3C and 3D. When $d_3$ is scaled to $sd_3$ with $d_4$, $d_1$, and $d_2$ kept constant, the amplitude and period are extended as $s$ is decreased. When $s \lesssim 0.5$, the oscillations disappear as the system is caught at the $X \approx 1$ state losing the negative feedback destabilization of the $X \approx 1$ state. Similar behaviors were found when the structure-ATPase coupling was changed to $sd_4$ with $d_3$, $d_1$, and $d_2$ kept constant. Thus, the ATPase reactions give similar effects to the negative feedback in the present model. With the combined change to $sd_3$ and $sd_4$, the period change is more prominent, ranging from 9 h to 120 h (Fig 3C), which explains the observed ten-times period change induced by the single-residue substitution at the CI-CII interface [26]. Modifying the positive feedback strength to $sd_1$ and $sd_2$ shows that the oscillations disappear when the positive feedback is too weak or too strong (Fig 3D). The period and amplitude are enlarged as $s$ increases in between these boundaries of positive feedback strength (Fig 3C).

## Thermal loosening of the strcutural coupling explains temperature compensation

We propose that the increased structural fluctuations of KaiC in the higher temperature should weaken the interactions at the CI-CII interface to decrease $d_3$ and $d_4$ in Eq 4, producing similar effects to the single-residue substitution (Fig 3A). These effects should enlarge the amplitude and period, compensating for the accelerated reactions in high temperatures. Here, we examine our hypothesis by simulating the oscillations in various temperatures.

Assuming that the fluctuations are proportinal to exp(-$\Delta E_f/(k_B T)$) with a constant $\Delta E_f$, the feedback coupling strength at temperature $T$, $d_3(T)$ and $d_4(T)$, should be modified from those

in the standard temperature $T_0 = 30°C$ as $d_3(T) = d_3(T_0)/s(E_f; T, T_0)$ and $d_4(T) = d_4(T_0)/s(E_f; T, T_0)$;

$$s(\Delta E_f; T, T_0) = \exp(-\Delta E_f/(k_B T) + \Delta E_f/(k_B T_0)). \tag{6}$$

We call this temperature dependence of $d_3(T)$ and $d_4(T)$ Rule 1. Another rule comes from the activation energy $\Delta E_{gs \to fs} > 0$ and $\Delta E_{fs \to gs} > 0$ for the KaiB fold transformations. We assume $h_B \propto \exp[-\Delta E_{gs \to fs}/(k_B T)]$ and $f_B \propto \exp[-\Delta E'_{fs \to gs}/(k_B T)]$, which affects the binding/unbinding kinetics of KaiB. Here, $\Delta E'_{fs \to gs} = \Delta E_{fs \to gs} + \Delta E_{bound}$ and $\Delta E_{bound}$ is the KaiC-KaiB binding energy. We call this assumption on $h_B$ and $f_B$ Rule 2. The other assumption corresponds to the temperature insensitivity of the ATPase reactions as observed in experiments [23, 68]. We assume the temperature-insensitive ATPase reactions by imposing $\Delta^0_{ADP}(T) = \Delta^0_{ADP}(T_0)$ and $f_{hyd}(T) = f_{hyd}(T_0)$, where $\Delta^0_{ADP}(T)$ is a constant to determine the lifetime of the ADP bound state (Eq 3), and $f_{hyd}(T)$ is the hydrolysis frequency of the bound ATP. We call this assumption Rule 3. These three rules are summarized in Table 1.

The model has six rate constants (Table 2) other than the four rate constants, $h_B, f_B, \Delta^{0\ -1}_{ADP}$, and $f_{hyd}$, discussed in Table 1. Each of six rate constants should depend on temperature in each distinctive way. However, for examining the hypothesis transparently, we assume a straightforward case of the same activation energy $\Delta E_0$ in six rate constants, which leads to the same temperature dependence as $k_{dp}(T) = s(\Delta E_0; T, T_0)k_{dp}(T_0)$, etc., where $s$ is defined in Eq 6. In the case we do not impose any of Rule 1, Rule 2, or Rule 3 by assuming $\Delta^{0\ -1}_{ADP}(T) = s(\Delta E_0; T, T_0)\Delta^{0\ -1}_{ADP}(T_0)$ and $f_{hyd}(T) = s(\Delta E_0; T, T_0)f_{hyd}(T_0)$, all 10 rate constants are scaled in the same way, which is almost the same as the scaling in time units, making the oscillation period approximately proportional to $s(\Delta E_0; T, T_0)^{-1}$. This homogeneous activation without thermal attenuation of feedback should result in $Q_{10} = (\text{period in } T_0 - 5°C)/(\text{period in } T_0 + 5°C) \approx s(\Delta E_0; T_0 + 5, T_0 - 5) \approx 1.4$ for $\Delta E_0 = 10k_B T_0$ and $Q_{10} \approx 2$ for $\Delta E_0 = 20k_B T_0$. The purpose of the present subsection is to show that $|Q_{10} - 1| \lesssim 0.1$, or the oscillations are temperature compensated when we assume the three rules in Table 1 even in the case $\Delta E_0 = 10k_B T_0$ in other six rate constants. We also show that Rule 1 plays a dominant role, and temperature compensation is realized without imposing Rule 2 or 3; temperature compensation is realized if Rule 1 is satisfied even when $\Delta E_0 = 10k_B T_0$ is used for all ten rate constants.

**Table 1. Temperature dependence/independence of specific parameters.**

| Rules | $T$-dependence* | Physical implications |
|---|---|---|
| Rule 1 | $d_3(T) = \dfrac{d_3(T_0)}{s(\Delta E_f; T, T_0)}$ | Thermally attenuated structure-P/dP feedback |
| | $d_4(T) = \dfrac{d_4(T_0)}{s(\Delta E_f; T, T_0)}$ | Thermally attenuated structure-ATPase coupling |
| Rule 2 | $h_B(T) \propto s(\Delta E_0; T, T_0)\, s(\Delta E_{gs \to fs}; T, T_0)$ | Thermally activated KaiB fold |
| | $f_B(T) \propto s(\Delta E_0; T, T_0)\, s(\Delta E'_{fs \to gs}; T, T_0)$ | |
| Rule 3 | $\Delta^0_{ADP}(T) = \Delta^0_{ADP}(T_0)$ | $T$-insensitive lifetime of the ADP bound state |
| | $f_{hyd}(T) = f_{hyd}(T_0)$ | $T$-insensitive frequency of ATP hydrolysis |
| Case A | Rule 1+Rule 2+Rule 3 | |
| Case B | Rule 1+Rule 3 | $\Delta E_{gs \to fs} = \Delta E'_{fs \to gs} = 0$ |
| Case C | Rule 1+Rule 2 | $\Delta^0_{ADP}(T)^{-1} \propto s(\Delta E_0; T, T_0)$ |
| | | $f_{hyd}(T) \propto s(\Delta E_0; T, T_0)$ |
| Case D | Rule 2+Rule 3 | $\Delta E_f = 0$ |

*$T_0 = 30°C$, $\Delta E_0 = 10k_B T_0$, $\Delta E_f = 7k_B T_0$, $\Delta E_{gs \to fs} = 10k_B T_0$, and $\Delta E'_{fs \to gs} = 12k_B T_0$.

**Table 2. Rate constants in the model.**

| Constants | Standard values ($h^{-1}$)* | Reactions | Equations |
|---|---|---|---|
| $h_{A0}$ | $5 \times 10^{-1}$ | KaiA binding to KaiC | Eq 18 |
| $f_{A0}$ | $1 \times 10^{3}$ | KaiA unbinding from KaiC | Eq 18 |
| $h_{B0}$ | $5 \times 10^{-5}$ | KaiB binding to KaiC | Eqs 22 and 23, |
| $f_{B0}$ | $2$ | KaiB unbinding from KaiC | Eq 22 |
| $h_{AB}$ | $6 \times 10^{-1}$ | KaiA binding to KaiB | Eqs 19 and 20 |
| $f_{AB}$ | $1 \times 10^{2}$ | KaiA unbinding from KaiB | Eqs 19 and 20 |
| $k_{P}$ | $0.18$ | Phosphorylation (P) | Eq 24 |
| $k_{dp}$ | $0.18$ | Dephosphorylation (dP) | Eq 24 |
| $f_{hyd}$ | $1$ | Hydrolysis freq. of the bound ATP | Eq 26 |
| ${\Delta_{ADP}^{0}}^{-1}$ | $1$ | 1/(lifetime) of the bound ADP | Eq 27 |

* Values defined at $T = T_0$. Concentrations are defined in units of $V = 1$.

In order to distinguish the roles of three rules, we examined four cases (Table 1). All three Rules apply in Case A (Fig 4A), Rules 1 and 3 in Case B (Fig 4B), Rules 1 and 2 in Case C (Fig 4C), and Rules 2 and 3 in Case D (Fig 4D). The period is temperature compensated in Case A ($Q_{10} = 1.01$), Case B ($Q_{10} = 0.93$), and Case C ($Q_{10} = 1.02$) with a slight overcompensation in Case B, while the period shows a distinct temperature dependence in Case D ($Q_{10} = 1.51$), showing that Rule 1 plays a dominant role in temperature compensation. The overcompensation in Case B shows that Rule 2 enhances the temperature dependence of the period, which was compensated for by Rule 1 in Cases A and C. In Cases A, B, and C, amplitude sharply decreases as temperature decreases below 20˚C as observed experimentally [69]. We should
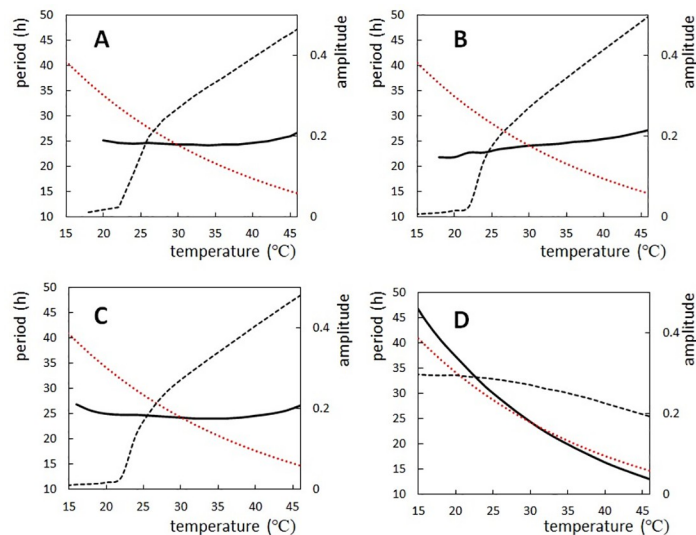


**Fig 4. Temperature dependence of the period and amplitude of the simulated oscillations.** Period (solid line) and amplitude (dashed line) of the ensemble-averaged phosphorylation level $\bar{D}(t)$ were calculated as functions of temperature with various modeling rules. Compared is the relative change of 1/rate of the process having the $10 k_B T_0$ activation energy (red dotted line). (**A**) Rule 1 (thermal attenuation of the negative feedback coupling), Rule 2 (thermal transformation of KaiB to a bindable conformation), and Rule 3 (temperature-insensitive ATPase reactions) applied (Case A). (**B**) Rule 1 and Rule 3 applied (Case B). (**C**) Rule 1 and Rule 2 applied (Case C). (**D**) Rule 2 and Rule 3 applied (Case D). $N = 2000$.
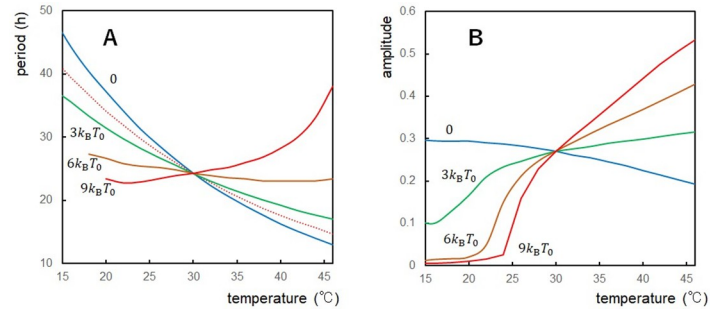
**Fig 5. Temperature dependence of the period and amplitude simulated with a different activation energy of structural fluctuations.** Period and amplitude of the ensemble-averaged phosphorylation level $\bar{D}(t)$ were calculated with various values of the activation energy of structural fluctuations $\Delta E_f$ with $\Delta E_f = 0$ (blue), $3k_B T_0$ (green), $6k_B T_0$ (brown), and $9k_B T_0$ (red) with $T_0 = 30°$C. (**A**) Period plotted for each $\Delta E_f$ as a function of temperature. Compared is the relative change of 1/rate of the process having the $10k_B T_0$ activation energy (red dotted line). (**B**) Amplitude plotted for each $\Delta E_f$ as a function of temperature. $N = 2000$.

note that Rule 3, temperature insensitivity of ATPase reactions, does not play a significant role in the present examination (Fig 4C); we discuss more on this point in the "Effects of the ATPase reactions" subsection.

A determinant role of Rule 1 is evident also from calculations with the varied temperature dependence of the structural fluctuations. $Q_{10}$ decreases as $\Delta E_f$ increases (Fig 5A); $Q_{10} = 1.51$ ($\Delta E_f = 0$), 1.28 ($\Delta E_f = 3k_B T_0$), 1.08 ($\Delta E_f = 6k_B T_0$), and 0.90 ($\Delta E_f = 9k_B T_0$); showing the temperature compensation with $6k_B T_0$, and the distinct overcompensation with $9k_B T_0$. A drop of the amplitude in the low temperature regime takes place at the higher temperature as $\Delta E_f$ increases (Fig 5B), consistently with the expected period-amplitude correlation.

Fig 5 shows a sensitive dependence of $Q_{10}$ on $\Delta E_f$. In KaiC mutants showing the altered oscillation period, we can expect the intact $Q_{10} \approx 1$ when the mutations perturb the P/dP-reaction rates in the CII or the ATPase-reaction rates in the CI, which alters the period, but does not alter the CI-CII interface, and hence does not affect $\Delta E_f$ much. However, with a single-residue substitution at the CI-CII interface of KaiC, the substitution can change $\Delta E_f$. In the experimental report, some substitutions at the CI-CII interface showed the intact $Q_{10}$, but the others showed the enlarged $Q_{10}$ [26]. A possible explanation for the former case is that the protein region around the substituted residue compensates for the structural fluctuations' temperature dependence, leading to the robust $\Delta E_f$ against the mutation, while in the latter case, such compensation does not sufficiently work, leading to the enlarged $Q_{10}$. It is crucial to examine whether such a difference in $\Delta E_f$ indeed occurs in those mutants.

## Phase shift caused by a stepping change in temperature

A significant feature of circadian rhythms is the response of their oscillation phase to the external stimuli. In particular, the phase is distinctively shifted by a temperature change in circadian oscillators while their period is temperature compensated [70, 71]. Also, in the in vitro KaiABC system, Yoshida et al. [72] found the phase shift indued upon temperature change. A step-up of temperature from $T = 30°$C to $45°$C in the dP process advanced the phase, while a step-up in the P process delayed the phase. On the other hand, a step-down of temperature from $T = 45°$C to $30°$C in the P process advanced the phase, and a step-down in the dP process delayed the phase. Here, we compare the simulated phase shift in the present model with the experimental results in [72]. In order to avoid the confusion coming from the slight period change upon temperature stepping, we defined the circadian time (CT) in the same way as in
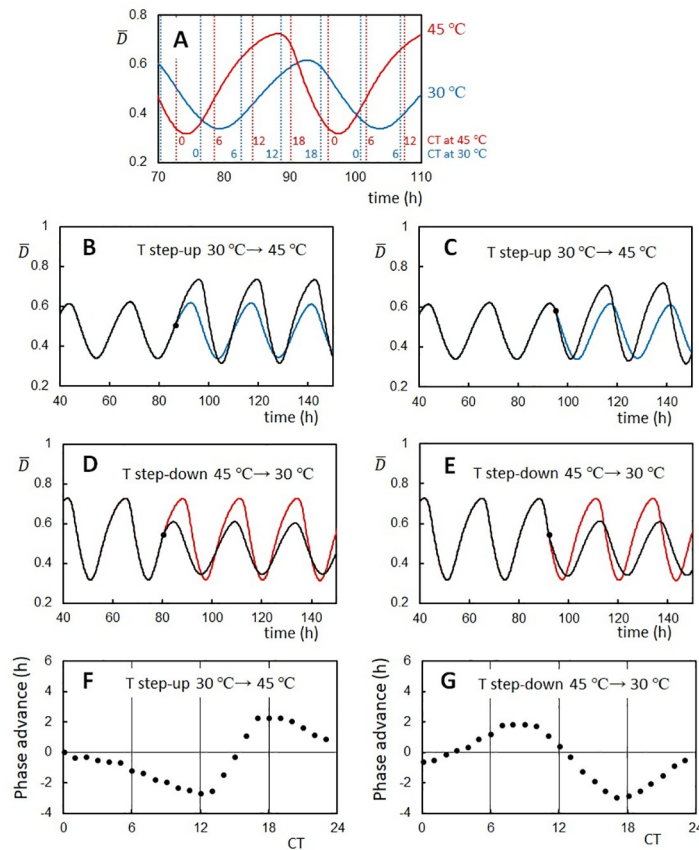
**Fig 6. Phase shifts of the ensemble-averaged oscillations of the KaiC phosphorylation level caused by temperature steps.** (**A**) Circadian Time (CT) was set to be 16 at the peak of oscillations at each temperature and the period was normalized to be 24 h in CT. Time denoted on the $x$-axis is the simulated incubation time (IT). (**B**) An example trajectory showing the phase delay upon temperature step-up from $T = 30˚C$ to $T = 45˚C$ at CT 9 (filled circle at IT 85.6 h). (**C**) An example trajectory showing the phase advance upon temperature step-up from $T = 30˚C$ to $T = 45˚C$ at CT 17.3 (filled circle at IT 95). In **B** and **C**, The oscillation trajectory going through the temperature step-up (black) and the trajectory with the constant temperature at $T = 30˚C$ (blue) are superposed. (**D**) An example trajectory showing the phase advance upon temperature step-down from $T = 45˚C$ to $T = 30˚C$ at CT 7.9 (filled circle at IT 80.4). (**E**) An example trajectory showing the phase delay upon temperature step-down from $T = 45˚C$ to $T = 30˚C$ at CT 20 (filled circle at IT 92). In **D** and **E**, The oscillation trajectory going through the temperature step-down (black) and the trajectory with the constant temperature at $T = 45˚C$ (red) are superposed. (**F**) Phase response curve (PRC) plotted as a function of CT when the temperature was stepped up from $T = 30˚C$ to $T = 45˚C$. (**G**) PRC plotted as a function of CT when the temperature was stepped down from $T = 45˚C$ to $T = 30˚C$. Rule 1, Rule 2, and Rule 3 in Table 1 were used with $\Delta E_0 = 6k_B T_0$ and $N = 1000$.

Ref. [72]: timing of the peak in the simulated rhythm at each temperature was set to CT 16, and the period length was normalized to be 24 h in CT (Fig 6A).

In the present model, oscillations of individual KaiC molecules are synchronized by the KaiA binding to the KaiC-KaiB-KaiA complexes, which entrains oscillating molecules in the ensemble into the dP phase [44]. With Rule 2 in Table 1, the $T$ step-down increases the ratio $h_B/f_B$, enhancing the entrainment and stabilizing the dP phase. Thus, the $T$ step-down in the dP phase elongates the dP process and causes the phase delay. On the other hand, the $T$ step-up in the same dP phase causes the opposite effect of the phase advance.

This expectation is confirmed in the results shown in Fig 6B–6G. In Fig 6B and 6C, the temperature was stepped up from $T = 30˚C$ to $45˚C$. Fig 6B shows the phase delay caused by a simulated $T$ step-up in the P phase at CT 9 (85.6 h in the simulated incubation time (IT)), and Fig

6C shows the phase advance caused by a $T$ step-up in the dP phase at CT 17.3 (IT 95). In Fig 6D and 6E, the temperature was stepped down from $T = 45°$C to $30°$C. Fig 6D shows the phase advance caused by a simulated $T$ step-down in the P phase at CT 7.9 (IT 80.4), and Fig 6E shows the phase delay caused by a $T$ step-down in the dP phase at CT 20 (IT 92). These results can be quantified by plotting a phase response curve (PRC). Fig 6F and 6G show PRCs for $T$ step-up and $T$ step-down, respectively. These simulated PRCs qualitatively reproduce the experimentally observed PRCs in [72]: upon $T$ step-up, the phase was advanced at CT 16–CT 22 and delayed at CT 8–CT 14, and upon $T$ step-down, the phase was advanced at CT 6–CT 11 and delayed at CT 14–CT 24. Thus, our model reproduces the essential features of the experimentally observed phase shift upon the stepping change of temperature.

## Effects of the ATPase reactions

In order to clarify the effects of the ATPase reactions on the oscillations, we scaled the rate constants of the ATPase reactions in the present model. Fig 7A shows the amplitude and period calculated by modifying the inverse lifetime of the ADP bound state, $\Delta_{\mathrm{ADP}}^{0}{}^{-1}$, and the hydrolysis frequency of the bound ATP, $f_{\mathrm{hyd}}$. They were scaled by a factor $s_a$ in two different ways; in case I, they were scaled as $s_a(\Delta_{\mathrm{ADP}}^{0})^{-1}$ and $s_a f_{\mathrm{hyd}}$, and in case II, $(s_a\Delta_{\mathrm{ADP}}^{0})^{-1}$ and $s_a f_{\mathrm{hyd}}$. In case I, period and amplitude only slightly depend on $s_a$ for $s_a > 0.5$. This insensitivity to the scaling corresponds to the temperature insensitivity shown in Fig 4C, where we did not use Rule 3 but scaled the constants as $\Delta_{\mathrm{ADP}}^{0}(T)^{-1} = s(\Delta E_0; T, T_0)\Delta_{\mathrm{ADP}}^{0}(T_0)^{-1}$ and $f_{\mathrm{hyd}}(T) = s(\Delta E_0; T, T_0)f_{\mathrm{hyd}}(T_0)$. The insensitivity in case I and Fig 4C indicates that the change in the ATPase reaction rates does not affect the period when they were changed with the constraint $\Delta_{\mathrm{ADP}} \cdot f_{\mathrm{hyd}} = $ const. The ATPase reactions should affect the period in two ways: The probability that the CI binds ADP during the P phase is correlated to how the $X \approx 1$ state is destabilized, and the probability that the CI binds ATP during the dP phase is correlated to how the $X \approx 0$ state is destabilized. However, changing the rates under the constraint $\Delta_{\mathrm{ADP}} \cdot f_{\mathrm{hyd}} = $ const does not affect these probabilities. Therefore, the period was insensitive to the changes in the rate constants under the constraint $\Delta_{\mathrm{ADP}} \cdot f_{\mathrm{hyd}} = $ const.

In case II, this constraint is not satisfied, and the change in the rate constants brings about a significant change in the period (Fig 7A). We examined the correlation between the oscillation frequency (i.e., 1/period) and the ATPase activity calculated in the nonoscillatory condition in
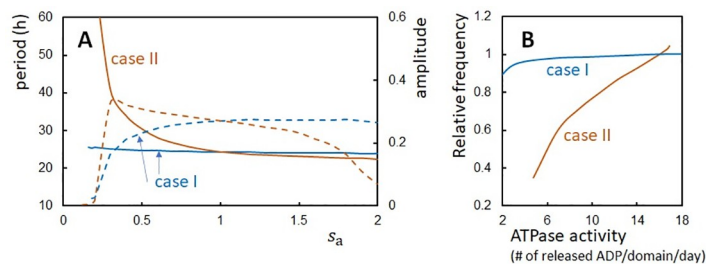


**Fig 7. Oscillations and the ATPase activity calculated with the modified rate constants of the ATPase reactions.** Two ways of the modification, case I and case II, were tested on the inverse lifetime of the ADP bound state, $\Delta_{\mathrm{ADP}}^{0}{}^{-1}$, and the frequency of hydrolysis of the bound ATP, $f_{\mathrm{hyd}}$. In case I (blue), the rate constants were scaled as $s_a(\Delta_{\mathrm{ADP}}^{0})^{-1}$ and $s_a f_{\mathrm{hyd}}$, and in case II (brown), $(s_a\Delta_{\mathrm{ADP}}^{0})^{-1}$ and $s_a f_{\mathrm{hyd}}$. **(A)** The period (solid line) and amplitude (dashed line) of the ensemble-averaged phosphorylation level $\bar{D}(t)$ were calculated as functions of $s_a$. **(B)** The frequency (inverse period) of oscillations of $\bar{D}(t)$ is compared with the ATPase activity (in units of the number of released ADP molecules from a CI domain in a day). The ATPase activity was calculated in the nonoscillatory condition in the absence of KaiA and KaiB. Temperature is $T_0$ and $N = 2000$.

the absence of KaiA and KaiB. Fig 7B shows a clear correlation between the oscillation frequency and the ATPase activity in case II as experimentally observed [23, 24]. The period is insensitive to the change in the ATPase rates only when the specific constraint is satisfied. This result suggests that the strategy to keep the specific constraint has been avoided in evolutionary design. Instead, the more general strategy of the temperature-insensitive ATPase reactions might have been evolutionarily realized in KaiC [23, 68] as in the TTO regulator, CKI$\varepsilon/\delta$, in mammals [22].

The present analysis showed that the oscillation period changes when $\Delta_{\mathrm{ADP}} \cdot f_{\mathrm{hyd}}$ varies; therefore, the temperature dependence of the period may be enhanced in mutants in which the temperature dependence of $\Delta_{\mathrm{ADP}}$ and/or $f_{\mathrm{hyd}}$ was modified, making $\Delta_{\mathrm{ADP}} \cdot f_{\mathrm{hyd}}$ dependent on temperature. Indeed, when $\Delta^0_{\mathrm{ADP}}(T)^{-1} = s(\Delta E_{\mathrm{a}}; T, T_0)\Delta^0_{\mathrm{ADP}}(T_0)^{-1}$ and $f_{\mathrm{hyd}}(T) = s(\Delta E_{\mathrm{b}}; T, T_0)f_{\mathrm{hyd}}(T_0)$ with $\Delta E_{\mathrm{a}} \neq \Delta E_{\mathrm{b}}$, the temperature dependence of the period should be enhanced. However, the temperature dependence of the structure-reaction coupling with $\Delta E_{\mathrm{f}} > 0$ at the CI-CII interface should compensate for this effect. For example, the present model calculation with $\Delta E_{\mathrm{a}} = 5k_{\mathrm{B}}T_0$, $\Delta E_{\mathrm{b}} = 0$, and $\Delta E_{\mathrm{f}} = 7k_{\mathrm{B}}T_0$ showed $Q_{10} = 1.04$, showing only a mild increase of $Q_{10}$ from $Q_{10} = 1.01$ in Fig 4A. However, with the larger temperature dependence of the ATPase activity as $\Delta E_{\mathrm{a}} = 10k_{\mathrm{B}}T_0$ and $\Delta E_{\mathrm{b}} = 0$ with $\Delta E_{\mathrm{f}} = 7k_{\mathrm{B}}T_0$, we have $Q_{10} = 1.06$; therefore, the further analyses are necessary for elucidating the relationship between the temperature dependence of the period and the temperature dependence of the ATPase activity. It is important to analyze how the $Q_{10}$ of the oscillation period varies among mutants showing the larger $Q_{10}$ of the ATPase activity [68].

## Phase shift caused by a pulse of the increased ADP concentration

Examining the response of the oscillation phase to the change in the ATP/ADP concentration ratio should further test the roles of the ATP hydrolyses in the KaiABC oscillations. Rust et al. [73] experimentally examined the phase response of the in vitro KaiABC system by adding ADP to the reaction buffer at various timing. After several hours of ADP addition, they reduced the ADP concentration to the original level by adding pyruvate kinase, which converts ADP to ATP. Rust et al. found that this pulse of ADP addition delayed the oscillation phase when the pulse was added at around the trough of the oscillating phosphorylation level, while the pulse advanced the phase when the pulse was added at around the peak of the phosphorylation level [73]. In our model, the increased concentration of ADP should elongate the ADP-bound state's lifetime, enhancing the transition probability from the P phase to the dP phase and reducing the probability of the opposite transition. Therefore, we expect that adding the ADP pulse at the oscillation peak helps the transition to advance the phase, while adding the ADP pulse at the oscillation trough disturbs the transition to delay the phase. This expectation is consistent with the results observed in [73], and we confirmed it with simulations as in the following.

In our model, the effects of an increase in the ADP concentration should correspond to the increase in the ADP-bound state's lifetime. Therefore, we simulated the ADP pulse by increasing $\Delta^0_{\mathrm{ADP}}$ at a particular time and reducing $\Delta^0_{\mathrm{ADP}}$ to the original value 6 hours after the increase. We defined CT in the same way as in Fig 6 (Fig 8A) and used the same parameters as in Fig 4A. Fig 8B and 8D show the example phase shift with the simulated addition of ADP pulse around the trough and the peak of oscillations, respectively. As expected, the addition of the pulse around the trough delayed the oscillation phase (Fig 8B), and the addition of the pulse around the peak advanced the phase (Fig 8D). It is intriguing that the simulated change from the phase-delay to phase-advancement behaviors was abrupt, inducing a jump in the PRC at around CT 5 (Fig 8E), reproducing the observed jump in the experimental PRC [73]. The
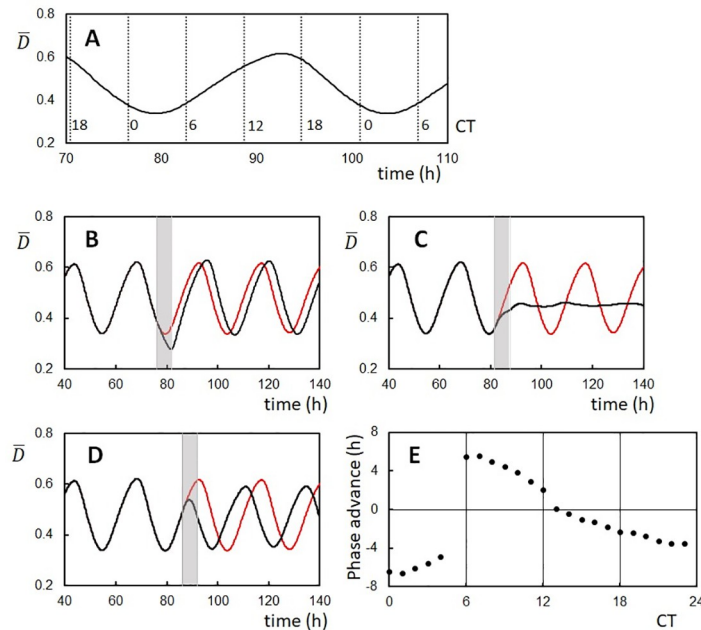
**Fig 8. Phase shifts of the ensemble-averaged oscillations of the KaiC phosphorylation level caused by pulses of the ADP increase.** (**A**) Circadian Time (CT) was set to be 16 at the peak of oscillations and the period was normalized to be 24 h in CT. Time denoted on the *x*-axis is the simulated incubation time (IT). (**B**) An example trajectory showing the phase delay by adding an ADP pulse from CT 0 to CT 6 (gray bar from IT 76 to IT 82). (**C**) An example trajectory showing the desynchronization by adding an ADP pulse from CT 5 to CT 11 (gray bar from IT 81.6 to IT 87.6). (**D**) An example trajectory showing the phase advance by adding an ADP pulse from CT 9.5 to CT 15.5 (gray bar from IT 86 to IT 92). In **B**, **C**, and **D**, the oscillation trajectory perturbed by an ADP pulse (black) and the trajectory without perturbation (red) are superposed. (**E**) PRC plotted as a function of CT when the ADP pulse started to be added. During the ADP pulse, $\Delta_{ADP}^0$ was increase to $4\Delta_{ADP}^0$. $T = T_0$ and $N = 1000$.

model predicts that the addition of the ADP pulse at the jump point at CT 5 (IT 81.6) advanced the oscillation phase of almost half of KaiC molecules and delayed the phase of the rest half of molecules, which strongly desynchronized the oscillations of individual KaiC molecules, diminishing the ensemble-level oscillations (Fig 8C); it is important to experimentally examine this desynchronization as a test of the oscillation mechanism proposed in the present model.

## Discussion

Using the model describing the feedback coupling among reactions and structural transitions in individual KaiC molecules and synchronization of many KaiC molecules, we showed that weakening the negative feedback strength extends the amplitude and lengthens the period of oscillations in the KaiABC system. This weakening can explain the observed wide range of period modification induced by the single-residue substitution at the CI-CII interface of KaiC [26]. We hypothesized that thermal fluctuations induce similar effects to the substitution at the CI-CII interface, which explained the stable temperature compensation in the KaiABC system. The ATPase reactions also affect the period, but the period is insensitive when the ATPase rates are changed under the specific constraint.

A possible test of the thermal weakening of the CI-CII structural coupling is to measure the temperature dependence of the thermal fluctuations of the interface residue with NMR or other spectroscopic methods. The model predicts that the temperature dependence of
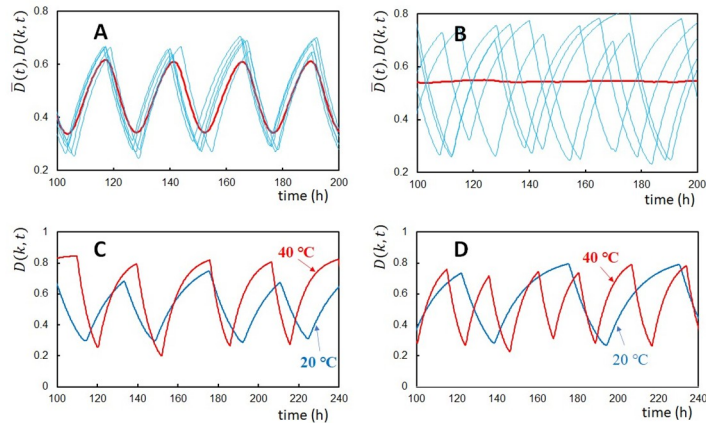
**Fig 9. Temperature compensation of oscillations of individual molecules.** In **A** and **B**, oscillations of the ensemble-averaged phosphorylation level $\bar{D}(t)$ (red) are compared with five individual oscillations $D(k, t)$ of molecules arbitrarily chosen from the ensemble (blue). $T = T_0$. (**A**) $h_{AB}$ was kept in the standard value (Table 2). (**B**) $h_{AB}$ was reduced to 1/20 of the standard value. (**C**) Oscillations of $D(k, t)$ of an arbitrarily chosen single molecule at $T = 40°$C (red) and $T = 20°$C (blue). Three rules, Rule 1 (thermal attenuation of the reaction-structure feedback coupling with $\Delta E_f = 6k_B T$), Rule 2 (thermal activation of KaiB transformation), and Rule 3 (temperature insensitivity of the ATPase reactions), were assumed. (**D**) Oscillations of $D(k, t)$ of an arbitrarily chosen single molecule at $T = 40°$C (red) and $T = 20°$C (blue). Rule 2 and Rule 3 were assumed, while Rule 1 was not adopted with $\Delta E_f = 0$. In **C** and **D**, $h_{AB}$ was reduced to 1/20 of the standard value. $N = 1000$.

fluctuations should be anti-correlated with the $Q_{10}$ of the period, and such an anti-correlation was suggested from the recent neutron scattering data [68].

Another possible test is to observe the single-molecular behavior. In the typical oscillatory condition, oscillations of individual KaiC molecules are synchronized, inducing coherent circadian oscillations at the ensemble level (Fig 9A). If the synchronization is realized through the sequestration of KaiA into the KaiC-KaiB-KaiA complexes as assumed in the present study, synchronization should be lost when the binding affinity between KaiA and KaiB is reduced. It would be possible to design a KaiB mutant with a low affinity to KaiA, and in the present model, such a mutant is represented by reducing the $h_{AB}$ value. With this reduction, synchronization is lost, and the ensemble oscillations disappear despite the oscillations with the large amplitude remaining in individual KaiC molecules (Fig 9B). In such a desynchronized condition, period of individual oscillations is temperature compensated with the temperature-dependent oscillation amplitude in the present model (Fig 9C). In contrast, when the negative feedback strength does not depend on temperature, individual oscillations are not temperature compensated without showing a significant temperature dependence of amplitude (Fig 9D). The temperature compensation hypothesis in the present study contrasts with the hypothesis of the competitive KaiA binding reactions [25]. With the latter hypothesis, temperature compensation is induced only from the ensemble level mechanism, not from the individual molecular mechanism, which should be distinguishable with the single-molecule observation in the condition that the synchronization is lost.

With the larger KaiA concentration than the standard value of $A_T/C_T = 1/3$, Ito-Miwa et al. showed that $Q_{10}$ of the oscillation period becomes large (Fig S6 in [26]). In our model with the parameters used in Fig 6, with the increased KaiA concentration of $A_T/C_T = 1/2$, the oscillation period was temperature compensated with $Q_{10} = 0.98$, which disagrees with the experimental report. We should note that the results depend on the parameterization in the model; for example, with $\Delta E_{gs \to fs} = 20k_B T$ and $\Delta E'_{fs \to gs} = 0$, $Q_{10} = 1.33$ when $A_T/C_T = 1/2$. Therefore, the

further examinations should be needed to compare the model results with the experimental report by carefully examining the mechanisms of the binding/unbinding kinetics of KaiA and KaiB to/from KaiC. Our analyses showed the importance of the molecular features which determine the coupling between reactions and structural transitions in the oscillating molecules. Investigations of the KaiABC system should highlight the significance of the regulation through the atomic reaction-structure coupling and help provide innovative methods of design for regulating the system dynamics of an ensemble of molecules.

## Methods

### Multifold feedback coupling in KaiC

We describe individual KaiC hexamers with coarse-grained variables; the binding state of KaiA on the CII domain, $\theta_{C_6A_2}(k)$, the binding state of KaiB and KaiA on the CI domain, $\theta_{C_6B_iA_{2j}}(k)$, the phosphorylation level, $0 \leq \mathcal{D}(k) \leq 1$, the structural state, $W(k)$, and the nucleotide-binding state, $q(i; k, t)$. Here,

$$\theta_{C_6A_2}(k) = \begin{cases} 1 & \text{(the CII of the $k$th KaiC binds KaiA)}, \\ 0 & \text{(otherwise)}, \end{cases} \tag{7}$$

$$\theta_{C_6B_iA_{2j}}(k) = \begin{cases} 1 & \text{(\# of KaiB and KaiA on the CI of the $k$th KaiC are $i$ and $j$)}, \\ 0 & \text{(otherwise)}, \end{cases} \tag{8}$$

$$W(k) = \begin{cases} 1 & \text{(strucutre in the P process)}, \\ -1 & \text{(structure in the dP process)}, \end{cases} \tag{9}$$

$$\mathcal{D}(k) = \text{(\# of phosphorylated sites in the $k$th KaiC)}/12, \tag{10}$$

$$q(i; k) = \begin{cases} 1 & \text{(the $i$th CI domain of the $k$th KaiC haxamer binds ADP)}, \\ 0 & \text{(the $i$th CI domain of the $k$th KaiC haxamer binds ATP)}. \end{cases} \tag{11}$$

We consider the system to consist of $N$ KaiC hexamers. Then, the system state at time $t$ is described by a set of vectors, $\vec{\theta}_{C_6A_2} = \{\theta_{C_6A_2}(1), \theta_{C_6A_2}(2), \cdots, \theta_{C_6A_2}(N)\}$, etc. The stochastic evolution of the system state is described by the probability distribution,

$$P_{\text{system}}(t) = P(\vec{\theta}_{C_6A_2}, \vec{\theta}_{C_6B_iA_{2j}}, \vec{\mathcal{D}}, \vec{W}, \vec{q}, x_A(t), x_B(t), t), \tag{12}$$

where $x_A(t)$ and $x_B(t)$ are concentrations of free KaiA dimer and KaiB monomer unbound from KaiC, respectively. The structural change takes place in milliseconds or so in usual protein oligomers, and we assume a similar timescale in the present problem. This timescale is much shorter than the timescales of other reactions; therefore, we treat the variable $\vec{W}$ as in quasi-equilibrium. Then, the quasi-equilibrium free energy $G_{\text{quasi}}$ should be expanded by $\vec{W}$ as $G_{\text{quasi}} = G_0 + \Sigma_k W(k)G_1(k) + \Sigma\Sigma_{k \neq l} W(k)W(l)G_2(k, l) + \cdots$. Here, because $W(k)^2 = 1$, the second-order term of the expansion only consists of the sum with $k \neq l$. In the present model, the interaction between different KaiC hexamers is indirect through the KaiA sequestration; therefore, we can put $G_2(k, l) = 0$. Then, in the expression $G_{\text{quasi}} = G_0 + \Sigma_k W(k)G_1(k)$, $W(k)$ behaves like an Ising spin under the external field $R(k, t) = -G_1(k)$. Therefore, the average of $W(k)$ in

quasi-equilibrium is $\bar{W}(k, t) = \tanh(-\beta R(k, t))$. By intoducing the order parameter of structure, $0 \leq X(k, t) \leq 1$, as $X(k, t) = (\bar{W}(k, t) + 1)/2$, we have

$$X(k, t) = \frac{1}{2}(1 + \tanh(\beta R(k, t)), \tag{13}$$

showing the same form as in Eq 4 in the main text. Here, $\beta = 1/(k_B T)$ is inverse temperature, and $R(k, t)$ is a quasi-equilibrium constraint reflecting the chemical state of the KaiC hexamer at time $t$. The explicit form of $R(k, t)$ represents how the feedback relations among reactions and structure work in the system and is defined after the other variables in Eq 12 are transformed to an expression suitable to be handled.

We use the mean-field approximation; Eq 12 is approximated by factorizing $P$ into each degree of freedom as

$$\begin{aligned} P_{\text{system}}(t) = &\prod_{k=1}^{N} P(\theta_{C_6A_2}(k), X(k, t), \mathbf{q}(k, t), x_A(t), x_B(t), t) \\ &\times \prod_{k=1}^{N}\prod_{i=0}^{6}\prod_{j=1}^{i} P(\theta_{C_6B_iA_{2j}}(k), X(k, t), \mathbf{q}(k, t), x_A(t), x_B(t), t) \\ &\times \prod_{k=1}^{N} P(\mathcal{D}(k), X(k, t), \mathbf{q}(k, t), x_A(t), x_B(t), t), \end{aligned} \tag{14}$$

where $\mathbf{q}(k, t) = \{q(1; k, t), q(2; k, t), \cdots, q(6; k, t)\}$ is a six-dimensional vector representing the nucleotide-binding state of each of six CI domains in the $k$th hexamer. We represent the non-equilibrium consumption of ATP by treating $q(i; k, t)$ as a stochastic variable taking the value either 1 or 0 depending on whether the CI domain binds ADP or ATP (Eq 11). $X(k, t)$, $x_A(t)$, and $x_B(t)$ are calculated by solving the relations explained in the subsections "Reaction-structure feedback coupling" and "Coupling of multiple oscillators" in this Methods section. Thus, by dropping the variables, $\mathbf{q}(k, t)$, $X(k, t)$, $x_A(t)$, and $x_B(t)$ from the expression, Eq 14 is

$$P_{\text{system}}(t) = \prod_{k=1}^{N}\left[P(\theta_{C_6A_2}(k), t)\left(\prod_{i=0}^{6}\prod_{j=1}^{i} P(\theta_{C_6B_iA_{2j}}(k), t)\right)P(\mathcal{D}(k), t)\right]. \tag{15}$$

$P_{\text{system}}(t)$ should obey the master equation representing reactions in the Kai system. In the mean-field approximation, the master equation is reduced to simpler equations similar to the chemical kinetics equations [74, 75]. Thus, we consider the equation of KaiA binding/unbinding kinetics for $P(\theta_{C_6A_2}(k), t)$, the equations of KaiB and KaiA binding/unbinding kinetics for $P(\theta_{C_6B_iA_{2j}}(k), t)$, and the equation of P/dP kinetics for $P(\mathcal{D}(k), t)$.

**KaiA and KaiB binding/unbinding kinetics.** Writing $P_{C_6A_2}(k, t) = P(\theta_{C_6A_2}(k) = 1, t)$, we have the kinetic equation for the KaiA binding and unbinding,

$$\frac{d}{dt}P_{C_6A_2}(k, t) = h_A x P_{C_6B_0A_0}(k, t) - f_A P_{C_6A_2}(k, t). \tag{16}$$

Because the KaiA binding and unbinding reactions are faster than the other reactions in the present system, we can approximate Eq 16 with the quasi-equilibrium approximation as $\frac{d}{dt}P_{C_6A_2}(k, t) = 0$. Then, we have

$$P_{C_6A_2}(k, t) = x_A(t)\, g_{C:A}(k, t) P_{C_6B_0A_0}(k, t), \tag{17}$$

with $g_{C:A}(k, t) = h_A(k, t)/f_A(k, t)$. As discussed in the main text, $h_A$ should be an increasing

function of $X(k, t)$ and $f_A$ is a decreasing function of $X(k, t)$. We use the form,

$$h_A(k, t) = h_{A0}\left[1 + \tanh\left(\frac{2X(k, t) - 1}{A_X}\right)\right],$$

$$f_A(k, t) = f_{A0}\left[1 - \tanh\left(\frac{2X(k, t) - 1}{A_X}\right)\right], \tag{18}$$

where $h_{A0}$ and $f_{A0}$ are the rate cosnstants to determine the time scale and $A_X > 0$ is a constant to determine the sensitvity to the structure.

In a similar way, by writing $P_{C_6B_iA_{2j}}(k, t) = P(\theta_{C_6B_iA_{2j}}(k) = 1, t)$, the binding and unbinding of KaiA to and from KaiB should be in quasi-equilibrium, leading to

$$P_{C_6B_iA_{2j}}(k, t) = x_A(t)\, g_{CB:A} P_{C_6B_iA_{2(j-1)}}(k, t), \tag{19}$$

with $g_{CB:A} = h_{AB}/f_{AB}$, where $h_{AB}$ and $f_{AB}$ are constants independent of $X(k, t)$. Then, we can write

$$P_{C_6B_iA_{2j}}(k, t) = \frac{i!}{j!(i-j)!}\alpha^j(1-\alpha)^{i-j}P_{C_6B_i}(k, t), \tag{20}$$

with $\alpha = \frac{x_A(t)g_{CB:A}}{1+xg_{CB:A}}$, and $P_{C_6B_i}(k, t) = \sum_{j=0}^{i} P_{C_6B_iA_{2j}}(k, t)$ for $i \geq 1$. Using the variables $P_{C_6B_i}(k, t)$, the kinetic equation for $P_{C_6B_iA_{2j}}(k, t)$ becomes

$$
\begin{aligned}
\frac{d}{dt}P_{C_6B_i}(k, t) &= (7-i)h_B x_B(t)P_{C_6B_{i-1}}(k, t) - if_B P_{C_6B_i}(k, t) \\
&\quad -(6-i)h_B x_B(t)P_{C_6B_i}(k, t) + (i+1)f_B P_{C_6B_{i+1}}(k, t), \quad \text{for } 1 \leq i \leq 5, \\
\frac{d}{dt}P_{C_6B_0}(k, t) &= -6h_B x_B(t)P_{C_6B_0}(k, t) + f_B P_{C_6B_1}(k, t), \\
\frac{d}{dt}P_{C_6B_6}(k, t) &= h_B x_B(t)P_{C_6B_5}(k, t) - 6f_B P_{C_6B_6}(k, t),
\end{aligned} \tag{21}
$$

where $P_{C_6B_0}(k, t) = P_{C_6A_2}(k, t) + P_{C_6B_0A_0}(k, t)$, and the rate constants are

$$h_B(k, t) = h_{B0}\left[1 - \tanh\left(\frac{2X(k, t) - 1}{B_X}\right)\right],$$

$$f_B(k, t) = f_{B0}\left[1 + \tanh\left(\frac{2X(k, t) - 1}{B_X}\right)\right]. \tag{22}$$

Here, $h_{B0}$ and $f_{B0}$ are the rate constants defining the time scale and $B_X > 0$ is a constant determining the sensitivity to the structure. Because the bindable conformation of KaiB appears with the thermal activation with the energy $\Delta E_{fs \to gs}$, we assume $h_{B0}$ and $f_{B0}$ at temperature $T$ are

$$h_{B0}(T) = h_{B0}(T_0)\exp\left(-\frac{\Delta E_0 + \Delta E_{fs \to gs}}{k_B T} + \frac{\Delta E_0 + \Delta E_{fs \to gs}}{k_B T_0}\right),$$

$$f_{B0}(T) = f_{B0}(T_0)\exp\left(-\frac{\Delta E_0 + \Delta E'_{gs \to fs}}{k_B T} + \frac{\Delta E_0 + \Delta E'_{gs \to fs}}{k_B T_0}\right), \tag{23}$$

as explained in Table 1 in the main text.

**P/dP kinetics.** For the P/dP reactions, we calculate $D(k,t) = \sum_{\mathcal{D}} \mathcal{D} P(\mathcal{D}(k),t)$. Then, we have

$$\frac{d}{dt}D(k,t) = k_{\mathrm{p}}H^+(k,t)[1 - D(k,t)] - k_{\mathrm{dp}}H^-(k,t)D(k,t), \tag{24}$$

with the rate constants $k_{\mathrm{p}}$ and $k_{\mathrm{dp}}$. Here, $H^+(k,t) = z/(1+z)$ and $H^-(k,t) = 1/(1+z)$ are the effects of binding and unbinding of KaiA to and from the CII, respectively, and $z = P_{\mathrm{C_6A_2}}(k,t)/P_0$ with a constant $P_0$.

**ATPase reactions.** We describe the non-equilibrium ATPase reactions by using a stochastic variable $q(i;k,t)$. When ATP is bound on the $i$th CI domain of the $k$th KaiC hexamer, we write $q(i;k,t) = 0$. The ATP hydrolysis is represented by the transition from $q(i;k,t) = 0$ to $q(i;k,t) = 1$, which takes place at a random timing with the frequency $f_{\mathrm{hyd}}$. We approximate that $f_{\mathrm{hyd}}$ does not depend on $X$, as explained in the main text. The state $q(i;k,t) = 1$ represents the ADP-bound state. It is not known how the release of inorganic phosphate (P$_i$) impacts the KaiC structure. In the present study, for simplicity, we do not distinguish the ADP+P$_i$ bound state just after the hydrolysis and the ADP bound state after the P$_i$ release. We assume that the lifetime of the ADP bound state $\hat{\Delta}_{\mathrm{ADP}}(k,t)$ is stochastically fluctuating as

$$\hat{\Delta}_{\mathrm{ADP}}(k,t) = \Delta_{\mathrm{ADP}}(k,t) + \xi(k,t), \tag{25}$$

where $\xi(k,t)$ is a random number satisfying $\langle \xi(k,t) \rangle = 0$ and $\langle \xi(k,t)\xi(k',t') \rangle = \delta_{kk'}\delta(t-t')\Delta_{\mathrm{ADP}}(k,t)$. After the ADP release, the ATP rebinds, which turns the nucleotide-binding state from $q(i;k,t) = 1$ to 0. As explained in the main text, we assume

$$f_{\mathrm{hyd}} = \mathrm{const.} \tag{26}$$

and

$$\Delta_{\mathrm{ADP}}(k,t) = \Delta_{\mathrm{ADP}}^0 \left[ 1 - \tanh\left( \frac{2X(k,t) - 1}{C_X} \right) \right], \tag{27}$$

where $C_X$ and $\Delta_{\mathrm{ADP}}^0$ are constants.

The ensemble-averaged rate of the ADP release, $\bar{q}_r(t)$, shown in Fig 2B, was calculated as

$$\bar{q}_r(t) = \frac{1}{\Delta t}\sum_{t \in \Delta t}\left( \frac{1}{6N}\sum_{k=1}^{N}\sum_{i=1}^{6}\theta[q(i;k,t-\delta t) - q(i;k,t)] \right), \tag{28}$$

where $\theta(x) = 1$ for $x > 0$ and $\theta(x) = 0$ for $x \le 0$. $\delta t = 10^{-3}$ h is the width of the simulation time step, and $\Delta t = 0.2$ h is the time window for the data sampling.

**Reaction-structure feedback coupling.** $R(k,t)$ in Eq 13 represents the major assumptions on the feedback coupling in the present model. We use $R(k,t) = d_0 + d_1 P_{\mathrm{C_6A_2}}(k,t) - d_2\sum_{i=0}^{6}\sum_{j=0}^{i}P_{\mathrm{C_6B_iA_{2j}}}(k,t) - d_3[D(k,t) - (1 - D(k,t))] - d_4 F(q(k,t))$ with constants $d_0$, $d_1$, $d_2$, $d_3$, and $d_4$, and

$$F(q(k,t)) = q(k,t)X(k,t) - (1 - q(k,t))(1 - X(k,t)). \tag{29}$$

Then, we have

$$X(k, t) = \frac{1}{2} \left\{ 1 + \tanh \left[ \beta \left( d_0 + d_1 P_{C_6 A_2}(k, t) - d_2 \sum_{i=0}^{6} \sum_{j=0}^{i} P_{C_6 B_i A_{2j}}(k, t) \right. \right. \right.$$

$$\left. \left. \left. - d_3 [D(k, t) - (1 - D(k, t))] - d_4 F(q(k, t)) \right) \right] \right\}. \tag{30}$$

**Coupling of multiple oscillators through conservation of molecules.** The constraints coming from the conservation of the total concentrations of KaiA (Eq 5 of the main text) and KaiB are simplified with the quasi-equilibrium treatment of KaiA (Eqs 17 and 19) as

$$x_A(t) \quad + \quad x_A(t) \left[ \frac{1}{V} \sum_{k=1}^{N} \frac{g_{C:A}(k, t)}{1 + x_A(t) g_{C:A}(k, t)} P_{C_6 B_0}(k, t) \right]$$

$$+ \quad \frac{x_A(t) g_{CB:A}}{1 + x_A(t) g_{CB:A}} \left[ \frac{1}{V} \sum_{k=1}^{N} \sum_{i=1}^{6} i P_{C_6 B_i}(k, t) \right] = A_T / 2, \tag{31}$$

$$x_B(t) + \frac{1}{V} \sum_{k=1}^{N} \sum_{i=1}^{6} i P_{C_6 B_i}(k, t) = B_T. \tag{32}$$

## Simulations

We simulated the system containing $N = 1000$ or 2000 KaiC hexamers by numerically integrating the kinetics with a time step of $\delta t = 10^{-3}$ h. The variables describing the system are $P_{C_6 A_2}(k, t)$, $P_{C_6 B_i A_{2j}}(k, t)$ $(0 \leq j \leq i \leq 6)$, $q(i; k, t)$ $(1 \leq i \leq 6)$, $D(k, t)$, $X(k, t)$, for $k = 1 \sim N$, $x_A(t)$ and $x_B(t)$. From given values of these variables at time $t$, the values at $t + \delta t$ were obtained by (i) stochastically updating $q(i; k, t)$ using constants $f_{hyd}$ and $\Delta_{ADP}^0$ with Eqs 25–27, (ii) evaluating the binding and unbinding constants of Eqs 18 and 22, (iii) updating $P_{C_6 A_2}(k, t)$ and $P_{C_6 B_i A_{2j}}(k, t)$ with Eqs 17, 20 and 21, (iv) updating $x_A$ and $x_B$ by solving Eqs 31 and 32, (v) updating $D(k, t)$ with Eq 24, and (vi) updating $X(k, t)$ using Eq 30. The period and amplitude were calculated from the trajectories, each having the length 3276.8 h obtained after the initial warming-up trajectories of 100 h length.

## Parameters

The KaiC concentration is $C_T = 3.3$ $\mu$M on a monomer basis for $N = 1000$ and $V = 3 \times 10^{-15} l$; this concentration is close to 3.5 $\mu$M, often used in experiments. We assume the ratio $A_T : B_T : C_T = 1 : 3 : 3$ as in many experiments [23, 54, 67]. The oscillations were robust against small parameter changes; therefore, we did not calibrate the parameters but determined them from the order of magnitude argument. We chose $h_{B0} B_T$ and $f_{B0}$ to satisfy $h_{B0} B_T \approx f_{B0} \approx 1 h^{-1}$. We used $h_{B0} = 5 \times 10^{-5}$ $h^{-1}$ and $f_{B0} = 2 h^{-1}$ in units of $V = 1$, corresponding to the dissociation constant of $K_d^{C:B} = 2.2 \times 10$ $\mu$M in $V = 3 \times 10^{-15} l$. We used $h_{A0} / f_{A0} = 5 \times 10^{-4}$ in units of $V = 1$, corresponding to $K_d^{C:A} = 1.1$ $\mu$M in $V = 3 \times 10^{-15} l$, which agrees with the experimentally observed values of $K_d^{C:A} \sim \mu$M [76]. The dissociation constant of KaiA and KaB was not yet observed experimentally. Here, we assumed a smaller value to ensure the sequestration effect; $g_{CB:A} = 6 \times 10^{-3}$ in units of $V = 1$, corresponding to $K_d^{CB:A} = 0.09$ $\mu$M in $V = 3 \times 10^{-15} l$.

**Table 3. Other parameters.**

| Constants | Standard values | Implications | Equations |
|---|---|---|---|
| $N$ | 1000 or 2000 | # of KaiC hexamers in the simulation | Eqs 31 and 32 |
| $\frac{B_T}{C_T/6}N$ | $6N$ | # of KaiB monomers in the simulation | Eqs 31 and 32 |
| $\frac{A_T/2}{C_T/6}N$ | $N$ | # of KaiA dimers in the simulation | Eqs 31 and 32 |
| $V$ | 1 | Volume in the simulation | Eqs 31 and 32 |
| $T_0$ | 30˚C | Standard temperature | |
| $\delta t$ | $10^{-3}$ h | Width of the simulation time step | |
| $d_0$ | $2k_B T_0$ | Determining the average structure | Eq 30 |
| $d_1$ | $5k_B T_0$ | Coupling strength of struct.-KaiA bind/unbind | Eq 30 |
| $d_2$ | $5k_B T_0$ | Coupling strength of struct.-KaiB bind/unbind | Eq 30 |
| $d_3$ | $3k_B T_0$ | Coupling strength of struct.-P/dP reactions | Eq 30 |
| $d_4$ | $2k_B T_0$ | Coupling strength of struct.-ATPase reactions | Eq 30 |
| $A_X$ | 1 | Sensitivity of KaiA binding to KaiC structure | Eq 18 |
| $B_X$ | 1 | Sensitivity of KaiB binding to KaiC structure | Eq 22 |
| $C_X$ | 2 | Sensitivity of ADP lifetime to KaiC structure | Eq 27 |
| $P_0$ | $1 \times 10^{-1}$ | Sensitivity of P/dP reactions to KaiA binding | Eq 24 |

https://doi.org/10.1371/journal.pcbi.1010494.t003

See Tables 2 and 3 for values of the other parameters. We chose $d_0$, $d_1$, $d_2$, $d_3$. and $d_4$ as of the order of $k_B T_0$, and $A_X$, $B_X$, and $C_X$ as of the order of one.

## Author Contributions

## References

1. Nakajima M, Imai K, Ito H, Nishiwaki T, Murayama Y, Iwasaki H, et al. Reconstitution of circadian oscillation of cyanobacterial KaiC phosphorylation in vitro. Science. 2005; 308(5720):414–415. https://doi.org/10.1126/science.1108451 PMID: 15831759

2. Akiyama S. Structural and dynamic aspects of protein clocks: how can they be so slow and stable? Cell Mol Life Sci. 2012; 69(13):2147–2160. https://doi.org/10.1007/s00018-012-0919-3 PMID: 22273739

3. Egli M. Intricate protein-protein interactions in the cyanobacterial circadian clock. J Biol Chem. 2014; 289(31):21267–21275. https://doi.org/10.1074/jbc.R114.579607 PMID: 24936066

4. Dunlap JC. Molecular bases for circadian clocks. Cell. 1999; 96(2):271–290. https://doi.org/10.1016/S0092-8674(00)80566-8 PMID: 9988221

5. Bell-Pedersen D, Cassone VM, Earnest DJ, Golden SS, Hardin PE, Thomas TL, et al. Circadian rhythms from multiple oscillators: lessons from diverse organisms. Nat Rev Genet. 2005; 6(7):544–556. https://doi.org/10.1038/nrg1633 PMID: 15951747

6. Pittendrigh CS. On temperature independence in the clock system controlling emergence time in *Drosophila*. Proc Natl Acad Sci U S A. 1954; 40(10):1018–1029. https://doi.org/10.1073/pnas.40.10.1018 PMID: 16589583

7. Hastings JW, Sweeney BM. On the mechanism of temperature independence in a biological clock. Proc Natl Acad Sci U S A. 1957; 43(9):804–811. https://doi.org/10.1073/pnas.43.9.804 PMID: 16590089

8. Lakin-Thomas P, Brody S, Coté GG. Amplitude model for the effects of mutations and temperature on period and phase resetting of the *Neurospora* circadian oscillator. J Biol Rhythms. 1991; 6(4):281–297. https://doi.org/10.1177/074873049100600401 PMID: 1837742

9. Ruoff P. Introducing temperature-compensation in any reaction kinetic oscillator model. J Interdiscipl Cycle Res. 1992; 23(2):92–99. https://doi.org/10.1080/09291019209360133

10. Ruoff P, Loros JJ, Dunlap JC. The relationship between FRQ-protein stability and temperature compensation in the *Neurospora* circadian clock. Proc Natl Acad Sci U S A. 2005; 102(49):17681–17686. https://doi.org/10.1073/pnas.0505137102 PMID: 16314576

11. Kurosawa G, Iwasa Y. Temperature compensation in circadian clock models. J Theor Biol. 2005; 233 (4):453–468. https://doi.org/10.1016/j.jtbi.2004.10.012 PMID: 15748908

12. Hong CI, Conrad ED, John J Tyson JT. A proposal for robust temperature compensation of circadian rhythms. Proc Natl Acad Sci U S A. 2007; 104(4):1195–1200. https://doi.org/10.1073/pnas.0601378104 PMID: 17229851

13. Leloup JC, Goldbeter A. Temperature compensation of circadian rhythms: Control of the period in a model for circadian oscillations of the per protein in *Drosophila*. Chronobiology Intern. 2009; 14(5):511–520. https://doi.org/10.3109/07420529709001472

14. Bodenstein C, Heiland I, Schuster S. Temperature compensation and entrainment in circadian rhythms. Phys Biol. 2012; 9(3):036011. https://doi.org/10.1088/1478-3975/9/3/036011 PMID: 22683844

15. François P, Despierre N, Siggia ED. Adaptive temperature compensation in circadian oscillations. PLoS Comp Biol. 2012; 8(7):e1002585. https://doi.org/10.1371/journal.pcbi.1002585 PMID: 22807663

16. Kidd PB, Young MW, Siggia ED. Temperature compensation and temperature sensation in the circadian clock. Proc Natl Acad Sci U S A. 2015; 112(46):E6284–E6292. https://doi.org/10.1073/pnas.1511215112 PMID: 26578788

17. Kurosawa G, Fujioka A, Koinuma S, Mochizuki A, Shigeyoshi Y. Temperature-amplitude coupling for stable biological rhythms at different temperatures. PLoS Comp Biol. 2017; 13:e1005501. https://doi.org/10.1371/journal.pcbi.1005501 PMID: 28594845

18. Avello P, Davis SJ, Ronald J, Pitchford JW. Heat the clock: entrainment and compensation in *Arabidopsis* circadian rhythms. J Circadian Rhythms. 2019; 17(1):5. https://doi.org/10.5334/jcr.179 PMID: 31139231

19. Avello P, Davis SJ, Pitchford JW. Temperature robustness in *Arabidopsis* circadian clock models is facilitated by repressive interactions, autoregulation, and three-node feedbacks. J Theor Biol. 2021; 509:110495. https://doi.org/10.1016/j.jtbi.2020.110495 PMID: 32966827

20. Ruoff P, Rensing L, Kommedal R, Mohsenzadeh S. Modeling temperature compensation in chemical and biological oscillators. Chronobiol Int. 1997; 14(5):499–510. https://doi.org/10.3109/07420529709001471 PMID: 9298285

21. Isojima Y, Naka jima M, Ukai H, Fujishima H, Yamada RG, Masumoto K, et al. CKIε/δ-dependent phosphorylation is a temperature-insensitive, period-determining process in the mammalian circadian clock. Proc Natl Acad Sci U S A. 2009; 106(37):15744–15749. https://doi.org/10.1073/pnas.0908733106 PMID: 19805222

22. Shinohara Y, Koyama YM, Ukai-Tadenuma M, Hirokawa T, Kikuchi M, G Yamada RG, et al. Temperature-sensitive substrate and product binding underlie temperature-compensated phosphorylation in the clock. Mol Cell. 2017; 67(5):783–798. https://doi.org/10.1016/j.molcel.2017.08.009 PMID: 28886336

23. Terauchi K, Kitayama Y, Nishiwaki T, Miwa K, Murayama Y, Oyama T, et al. ATPase activity of KaiC determines the basic timing for circadian clock of cyanobacteria. Proc Natl Acad Sci U S A. 2007; 104 (41):16377–16381. https://doi.org/10.1073/pnas.0706292104 PMID: 17901204

24. Abe J, Hiyama TB, Mukaiyama A, Son S, Mori T, Saito S, et al. Circadian rhythms. Atomic-scale origins of slowness in the cyanobacterial circadian clock. Science. 2015; 349(6245):312–316. https://doi.org/10.1126/science.1261040 PMID: 26113637

25. Hatakeyama TS, Kaneko K. Generic temperature compensation of biological clocks by autonomous regulation of catalyst concentration. Proc Natl Acad Sci U S A. 2012; 109(21):8109–8114. https://doi.org/10.1073/pnas.1120711109 PMID: 22566655

26. Ito-Miwa K, Furuike Y, Akiyama S, Kondo T. Tuning the circadian period of cyanobacteria up to 6.6 days by the single amino acid substitutions in KaiC. Proc Natl Acad Sci U S A. 2020; 117(34):20926–20931. https://doi.org/10.1073/pnas.2005496117 PMID: 32747571

27. Furuike Y, Mukaiyama A, Ouyang D, Ito-Miwa K, Simon D, Yamashita E, et al. Elucidation of master allostery essential for circadian clock oscillation in cyanobacteria. Sci Adv. 2022; 8(15):eabm8990. https://doi.org/10.1126/sciadv.abm8990 PMID: 35427168

28. Emberly E, Wingreen NS. Hourglass model for a proteinbased circadian oscillator. Phys Rev Lett. 2006; 96:038303. https://doi.org/10.1103/PhysRevLett.96.038303 PMID: 16486780

29. Mori T, Williams DR, Byrne MO, Qin X, Egli M, McHaourab HS, et al. Elucidating the ticking of an in vitro circadian clockwork. PLoS Biol. 2007; 5(4):e93. https://doi.org/10.1371/journal.pbio.0050093 PMID: 17388688

30. Yoda M, Eguchi K, Terada TP, Sasai M. Monomer-shuffling and allosteric transition in KaiC circadian oscillation. PLoS One. 2007; 2(5):e408. https://doi.org/10.1371/journal.pone.0000408 PMID: 17476330

31. Eguchi K, Yoda M, Terada TP, Sasai M. Mechanism of robust circadian oscillation of KaiC phosphorylation in vitro. Biophys J. 2008; 95(4):1773–1784. https://doi.org/10.1529/biophysj.107.127555 PMID: 18502804

32. Nagai T, Terada TP, Sasai M. Synchronization of circadian oscillation of phosphorylation level of KaiC in vitro. Biophys J. 2010; 98(11):2469–2477. https://doi.org/10.1016/j.bpj.2010.02.036 PMID: 20513390

33. Zhang D, Cao Y, Ouyang Q, Tu Y. The energy cost and optimal design for synchronization of coupled molecular oscillators. Nat Phys. 2019; 16(1):95–100. https://doi.org/10.1038/s41567-019-0701-7 PMID: 32670386

34. Takigawa-Imamura H, Mochizuki A. Predicting regulation of the phosphorylation cycle of KaiC clock protein using mathematical analysis. J Biol Rhythms. 2006; 21(5):405–416. https://doi.org/10.1177/0748730406291329 PMID: 16998160

35. van Zon JS, Lubensky DK, Altena PR, ten Wolde PR. An allosteric model of circadian KaiC phosphorylation. Proc Natl Acad Sci U S A. 2007; 104(18):7420–7425. https://doi.org/10.1073/pnas.0608665104 PMID: 17460047

36. Mori T, Sugiyama S, Byrne M, Johnson CH, Uchihashi T, Ando T. Revealing circadian mechanisms of integration and resilience by visualizing clock proteins working in real time. Nat Commun. 2018; 9 (1):3245. https://doi.org/10.1038/s41467-018-05438-4 PMID: 30108211

37. Rust MJ, Markson JS, Lane WS, Fisher DS, O'Shea EK. Ordered phosphorylation governs oscillation of a three-protein circadian clock. Science. 2007; 318(5851):809–812. https://doi.org/10.1126/science.1148596 PMID: 17916691

38. Wang J, Xu L, Wang E. Robustness and coherence of a three-protein circadian oscillator: Landscape and flux perspectives. Biophys J. 2009; 97(11):3038–3046. https://doi.org/10.1016/j.bpj.2009.09.021 PMID: 19948134

39. Phong C, Markson JS, Wilhoite CM, Rust MJ. Robust and tunable circadian rhythms from differentially sensitive catalytic domains. Proc Natl Acad Sci U S A. 2013; 110(3):1124–1129. https://doi.org/10.1073/pnas.1212113110 PMID: 23277568

40. Paijmans J, Lubensky DK, ten Wolde PR. A thermodynamically consistent model of the post-translational Kai circadian clock. PLoS Comput Biol. 2017; 13(3):e1005415. https://doi.org/10.1371/journal.pcbi.1005415 PMID: 28296888

41. Das S, Terada TP, Sasai M. Role of ATP hydrolysis in cyanobacterial circadian oscillator. Sci Rep. 2017; 7(1):17469. https://doi.org/10.1038/s41598-017-17717-z PMID: 29234156

42. Das S, Terada TP, Sasai M. Single-molecular and ensemble-level oscillations of cyanobacterial circadian clock. Biophys Physicobiol. 2018; 15:136–150. https://doi.org/10.2142/biophysico.15.0_136 PMID: 29955565

43. Sasai M. Effects of stochastic single-molecule reactions on coherent ensemble oscillations in the KaiABC circadian clock. J Phys Chem B. 2019; 123(3):702–713. https://doi.org/10.1021/acs.jpcb.8b10584 PMID: 30629448

44. Sasai M. Mechanism of autonomous synchronization of the circadian KaiABC rhythm. Sci Rep. 2021; 11(1):4713. https://doi.org/10.1038/s41598-021-84008-z PMID: 33633230

**45.** Nakajima M, Ito H, Kondo T. In vitro regulation of circadian phosphorylation rhythm of cyanobacterial clock protein KaiC by KaiA and KaiB. FEBS Lett. 2010; 584(5):898–902. https://doi.org/10.1016/j.febslet.2010.01.016 PMID: 20079736

**46.** Ito H, Kageyama H, Mutsuda M, Naka jima M, Oyama T, Kondo T. Autonomous synchronization of the circadian KaiC phosphorylation rhythm. Nat Struct Mol Biol. 2007; 14(11):1084–1088. https://doi.org/10.1038/nsmb1312 PMID: 17965725

**47.** Mori T, Saveliev SV, Xu Y, Stafford WF, Cox MM, Inman RB, et al. Circadian clock protein KaiC forms ATP-dependent hexameric rings and binds DNA. Proc Natl Acad Sci U S A. 2002; 99(26):17203–17208. https://doi.org/10.1073/pnas.262578499 PMID: 12477935

**48.** Hayashi F, Suzuki H, Iwase R, Uzumaki T, Miyake A, Shen JR, et al. ATP-induced hexameric ring structure of the cyanobacterial circadian clock protein KaiC. Genes to Cells. 2003; 8(3):287–296. https://doi.org/10.1046/j.1365-2443.2003.00633.x PMID: 12622725

**49.** Pattanayek R, Wang J, Mori T, Xu Y, Johnson CH, Egli M. Visualizing a circadian clock protein: crystal structure of KaiC and functional insights. Mol Cell. 2004; 15(3):375–388. https://doi.org/10.1016/j.molcel.2004.07.013 PMID: 15304218

**50.** Iwasaki H, Taniguchi Y, Ishiura M, Kondo T. Physical interactions among circadian clock proteins KaiA, KaiB and KaiC in cyanobacteria. EMBO J. 1999; 18(5):1137–1145. https://doi.org/10.1093/emboj/18.5.1137 PMID: 10064581

**51.** Chang YG, Kuo NW, Tseng R, LiWang A. Flexibility of the C-terminal, or CII, ring of KaiC governs the rhythm of the circadian clock of cyanobacteria. Proc Natl Acad Sci U S A. 2011; 108(35):14431–14436. https://doi.org/10.1073/pnas.1104221108 PMID: 21788479

**52.** Chang YG, Tseng R, Kuo NW, LiWang A. Rhythmic ring-ring stacking drives the circadian oscillator clockwise. Proc Natl Acad Sci U S A. 2012; 109(42):16847–16851. https://doi.org/10.1073/pnas.1211508109 PMID: 22967510

**53.** Murayama Y, Mukaiyama A, Imai K, Onoue Y, Tsunoda A, Nohara A, et al. Tracking and visualizing the circadian ticking of the cyanobacterial clock protein KaiC in solution. EMBO J. 2011; 30(1):68–78. https://doi.org/10.1038/emboj.2010.298 PMID: 21113137

**54.** Oyama K, Azai C, Nakamura K, Tanaka S, Terauchi K. Conversion between two conformational states of KaiC is induced by ATP hydrolysis as a trigger for cyanobacterial circadian oscillation. Sci Rep. 2016; 6:32443. https://doi.org/10.1038/srep32443 PMID: 27580682

**55.** Iwasaki H, Nishiwaki T, Kitayama Y, Naka jima M, Kondo T. KaiA-stimulated KaiC phosphorylation in circadian timing loops in cyanobacteria. Proc Natl Acad Sci U S A. 2002; 99(24):15788–15793. https://doi.org/10.1073/pnas.222467299 PMID: 12391300

**56.** Pattanayek R, Williams DR, Pattanayek S, Xu Y, Mori T, Johnson CH, et al. Analysis of KaiA-KaiC protein interactions in the cyano-bacterial circadian clock using hybrid structural methods. EMBO J. 2006; 25(9):2017–2028. https://doi.org/10.1038/sj.emboj.7601086 PMID: 16628225

**57.** Kitayama Y, Iwasaki H, Nishiwaki T, Kondo T. KaiB functions as an attenuator of KaiC phosphorylation in the cyanobacterial circadian clock system. EMBO J. 2003; 22(9):2127–2134. https://doi.org/10.1093/emboj/cdg212 PMID: 12727879

**58.** Xu Y, Mori T, Johnson CH. Cyanobacterial circadian clockwork: roles of KaiA, KaiB and the KaiBC promoter in regulating KaiC. EMBO J. 2003; 22(9):2117–2126. https://doi.org/10.1093/emboj/cdg168 PMID: 12727878

**59.** Kitayama Y, Nishiwaki-Ohkawa T, Sugisawa Y, Kondo T. KaiC intersubunit communication facilitates robustness of circadian rhythms in cyanobacteria. Nat Commun. 2013; 4:2897. https://doi.org/10.1038/ncomms3897 PMID: 24305644

**60.** Snijder J, Schuller JM, Wiegard A, Lössl P, Schmelling N, Axmann IM, et al. Structures of the cyanobacterial circadian oscillator frozen in a fully assembled state. Science. 2017; 355(6330):1181–1184. https://doi.org/10.1126/science.aag3218 PMID: 28302852

**61.** Pattanayek R, Egli M. Protein-protein interactions in the cyanobacterial circadian clock: structure of KaiA dimer in complex with C-terminal KaiC peptides at 2.8 Å resolution. Biochemistry. 2015; 54 (30):4575–4578. https://doi.org/10.1021/acs.biochem.5b00694 PMID: 26200123

**62.** Chang YG, Cohen SE, Phong C, Myers WK, Kim YI, Tseng R, et al. A protein fold switch joins the circadian oscillator to clock output in cyanobacteria. Science. 2015; 17(6245):324–328.

**63.** Henzler-Wildman K, Kern D. Dynamic personalities of proteins. Nature. 2007; 450:964–972. https://doi.org/10.1038/nature06522 PMID: 18075575

**64.** Mutoh R, Nishimura A, Yasui S, Onai K, Ishiura M. The ATP-mediated regulation of KaiB-KaiC interaction in the cyanobacterial circadian clock. PLoS One. 2013; 8(11):e80200. https://doi.org/10.1371/journal.pone.0080200 PMID: 24244649

65. Mukaiyama A, Furuike Y, Abe J, Yamashita E, Kondo T, Akiyama S. Conformational rearrangements of the C1 ring in KaiC measure the timing of assembly with KaiB. Sci Rep. 2018; 8(1):8803. https://doi.org/10.1038/s41598-018-27131-8 PMID: 29892030

66. Tseng R, Goularte NF, Chavan A, Luu J, Cohen SE, Chang YG, et al. Structural basis of the day-night transition in a bacterial circadian clock. Science. 2017; 355(6330):1174–1180. https://doi.org/10.1126/science.aag2516 PMID: 28302851

67. Nishiwaki T, Satomi Y, Kitayama Y, Terauchi K, Kiyohara R, Takao T, et al. A sequential program of dual phosphorylation of KaiC as a basis for circadian rhythm in cyanobacteria. EMBO J. 2007; 26 (17):4029–4037. https://doi.org/10.1038/sj.emboj.7601832 PMID: 17717528

68. Furuike Y, Ouyang D, Tominaga T, Matsuo T, Mukaiyama A, Kawakita Y, et al. Cross-scale analysis of temperature compensation in the cyanobacterial circadian clock system. Comm Phys. 2022; 5:75. https://doi.org/10.1038/s42005-022-00852-z

69. Murayama Y, Kori H, Oshima C, Kondo T, Iwasaki H, Ito H. Low temperature nullifies the circadian clock in cyanobacteria through Hopf bifurcation. Proc Natl Acad Sci U S A. 2017; 114(22):5641–5646. https://doi.org/10.1073/pnas.1620378114 PMID: 28515313

70. Glaser FT, Stanewsky R. Temperature synchronization of the *Drosophila* circadian clock. Curr Biol. 2005; 15(15):1352–1363. https://doi.org/10.1016/j.cub.2005.06.056 PMID: 16085487

71. Liu Y, Merrow M, Loros JJ, Dunlap JC. How temperature changes reset a circadian oscillation. Science. 1998; 281(5378):825–829. https://doi.org/10.1126/science.281.5378.825 PMID: 9694654

72. Yoshida T, Murayama Y, Ito H, Kageyama H, Kondo T. Nonparametric entrainment of the in vitro circadian phosphorylation rhythm of cyanobacterial KaiC by temperature cycle. Proc Natl Acad Sci U S A. 2009; 106(5):1648–1653. https://doi.org/10.1073/pnas.0806741106 PMID: 19164549

73. Rust MJ, Golden SS, O'Shea EK. Light-driven changes in energy metabolism directly entrain the cyanobacterial circadian oscillator. Science. 2011; 331(6014):220–223. https://doi.org/10.1126/science.1197243 PMID: 21233390

74. Sasai M, Wolynes PG. Stochastic gene expression as a manybody problem. Proc Natl Acad Sci U S A. 2003; 100:2374–2379. https://doi.org/10.1073/pnas.2627987100 PMID: 12606710

75. Walczak AM, Sasai M, Wolynes PG. Self-consistent proteomic field theory of stochastic gene switches. Biophys J. 2005; 88:828–850. https://doi.org/10.1529/biophysj.104.050666 PMID: 15542546

76. Kageyama H, Nishiwaki T, Nakajima M, Iwasaki H, Oyama T, Kondo T. Cyanobacterial circadian pacemaker: Kai protein complex dynamics in the KaiC phosphorylation cycle in vitro. Mol Cell. 2006; 23 (2):161–171. https://doi.org/10.1016/j.molcel.2006.05.039 PMID: 16857583